CHALMERS
UNIVERSITY OF TECHNOLOGY

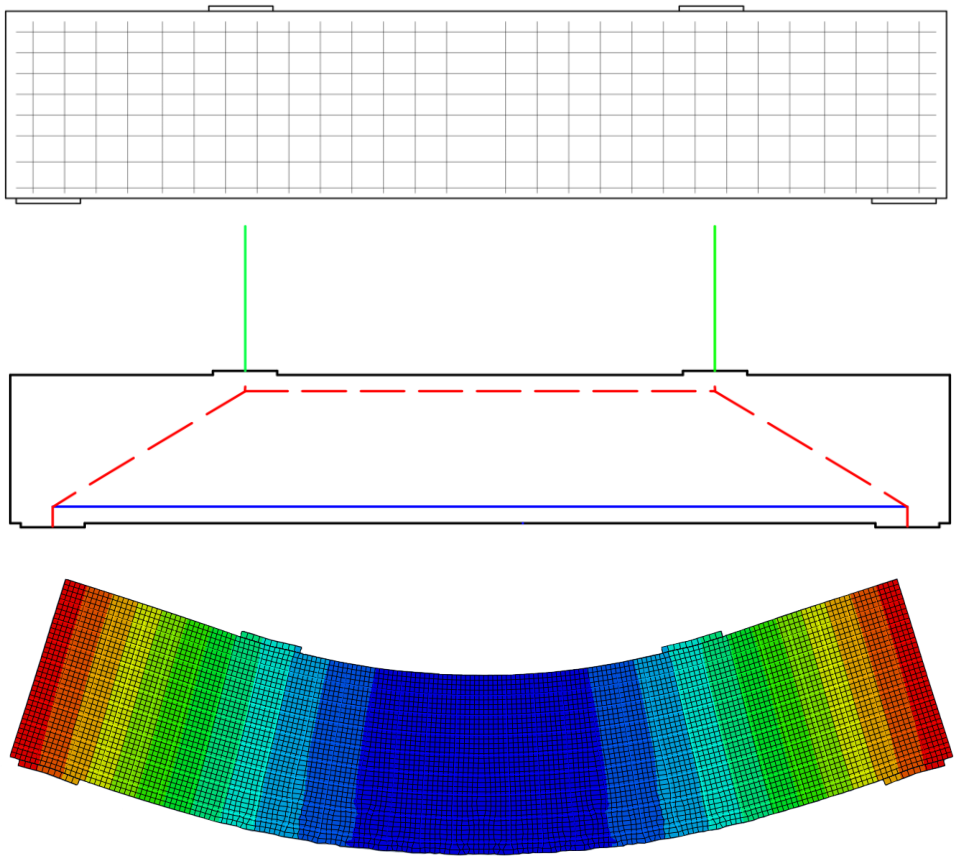

Comparison of structural analysis methods for reinforced concrete deep beams

Master's Thesis in the Master's Programme Structural Engineering and Building Technology

DENNIS WIKLUND

Department of Architecture and Civil Engineering
Division of Structural Engineering
Concrete Structures
CHALMERS UNIVERSITY OF TECHNOLOGY
Gothenburg, Sweden 2018
Master's Thesis ACEX30-2018: 102

MASTER'S THESIS ACEX30-2018: 102

Comparison of structural analysis methods for reinforced concrete deep beams

Master's Thesis in the Master's Programme Structural Engineering and Building Technology

DENNIS WIKLUND

Department of Architecture and Civil Engineering
Division of Structural Engineering
Concrete Structures
CHALMERS UNIVERSITY OF TECHNOLOGY
Göteborg, Sweden 2018

Comparison of structural analysis methods for reinforced concrete deep beams
Master's Thesis in the Master's Programme Structural Engineering and Building Technology

DENNIS WIKLUND

Examensarbete ACEX30-2018: 102/ Institutionen för bygg- och miljöteknik,
Chalmers tekniska högskola 2018

Department of Architecture and Civil Engineering
Division of Structural Engineering
Concrete Structures
Chalmers University of Technology
SE-412 96 Göteborg
Sweden
Telephone: + 46 (0)31-772 1000

Cover:
Figures of the ACI-I beam, see Section 3.1. The upmost figure displays a simple side-wise view, the middle figure shows an STM model from Mathcad analysis and the downmost figure shows from a non-linear FEM analysis from Abaqus.

Chalmers Reproservice
Göteborg, Sweden, 2018

Comparison of structural analysis methods for reinforced concrete beams

Master's thesis in the Master's Programme Structural Engineering and Building Technology

DENNIS WIKLUND
Department of Architecture and Civil Engineering
Division of Structural Engineering
Concrete Structures
Chalmers University of Technology

ABSTRACT

Structural engineers usually rely on traditional sectional models that are not fully valid when analyzing deep beams, for which other methods are available, like strut-and-tie method (STM) and finite element analysis (FEA). The aim of this study was to compare sectional models, STM, and non-linear FEA methods for analysis of reinforced concrete deep beams. This was done, to start, by reviewing existing literature, where examples of deep beams and accompanying test experiments could be found. Care was taken to make sure the deep beams differed in terms of geometry and reinforcement layout. The beams were first analyzed using sectional analysis and STM methods, as defined in Eurocode 2. Subsequently, the same beams were analyzed using non-linear FEA with the Abaqus CAE program. Finally, the results were extracted and compared. The comparison showed that both sectional analysis and STM modelling are quick and simple to implement, but only the latter is consistently accurate when it comes to analyzing the capacity of deep beams. Non-linear FEA is potentially more accurate and can demonstrate the simulated behavior of the deep beam over increasing load. It is, however, more complicated and time-consuming to implement.

Key words: Structural analysis, Reinforced concrete, Deep beams, Strut-and-tie model, Sectional methods, Finite element method, Resistance, Shear, Eurocode

Jämförelse av strukturella analysmetoder för armerade balkar

Examensarbete inom masterprogrammet Structural Engineering and Building Technology

DENNIS WIKLUND
Institutionen för arkitektur och samhällsbyggnadsteknik
Avdelningen för Arkitektur och teknik
Forskargrupp Armerad betong
Chalmers tekniska högskola

SAMMANFATTNING

Konstruktörer inom byggsektorn förlitar sig vanligtvis på traditionella tvärsnittsanalysmetoder, vilka inte alltid är giltiga när det gäller att analysera höga balkar. Istället finns andra tillgängliga metoder, såsom fackverksmetoden och finita-elementmetoden. Denna studies mål var att jämföra tvärsnittsanalys med fackverksmetoden och finita elementmetoden för analys av armerade höga betongbalkar. Detta gjordes, till att börja med, genom att genomsöka existerande litteratur, där exempel på höga balkar och belastningsförsök på sådana kunde hittas. Omsorg lades vid att se till att de höga balkarna varierade avseende geometri och armeringsutformning. Balkarna analyserades först med tvärsnitsanalys och fackverksmetoden såsom de är definierade i Eurocode 2. Därefter analyserades samma balkar med icke-linjär finit elementmetod med hjälp av programmet Abaqus CAE. Slutligen så jämfördes resultaten med varandra. Jämförelsen visade att både tvärsnittsanalysmetoden och fackverksmetoden är snabba och enkla att genomföra, men bara den sistnämnda är tillräckligt korrekt för att analysera höga balkars bärförmåga. Icke-linjär finit elementmetod är potentiellt mer exakt och kan simulera balkens simulerade beteende vid ökande belastning. Det är dock mer komplicerat och tidskrävande att använda denna metod.

Nyckelord: Strukturanalys, Armerad betong, Höga balkar, Fackversmetoden, Tvärsnittsanalys, Finita elementmetoden, Hållfasthet, Skjuvning

Contents

Preface

This thesis report has been made as the conclusive work of the MSc. Programme "Structural Engineering and Building Technology" at Chalmers University of Technology. The work has been carried out primarily in the spring of 2018 and at the Division of Structural Engineering, Research group Concrete Structures, Chalmers University of Technology, Sweden, and in cooperation with NCC.

The project was the idea of, and proposed by, doctoral students Adam Sciegaj and Alexandre Mathern (NCC). They also served as supervisors and their help was of great value to the project. Associate Professor PhD Mario Plos of Chalmers University of Technology served as the examiner.

Göteborg 2018

Dennis Wiklund

Acknowledgements

For their help in composing this report, I would like to extend my thanks to a number of different people. To start, for the invaluable advice and encouragement they provided over the making of this project, I extend the greatest amount of gratitude to both supervisors, Adam Sciegaj and Alexandre Marthern. The discussions and feedback they provided was instrumental to the realization of this project.

In addition, it should be noted that the simulations were performed on resources at Chalmers Centre for Computational Science and Engineering (C3SE) provided by the Swedish National Infrastructure for Computing (SNIC).

Also, special mention goes to Björn Engström, for being the main lecturer of the project's prerequisite concrete courses ('concrete structures' and 'structural concrete') at Chalmers University during my time of study, as well as for taking the time to attend a meeting with me and Alexandre Marthern during the early stages of the project.

Finally, I am grateful to all others that have offered their time and support, like Fahid Aslam, Ph. D at King Saud University, my examiner, Professor Mario Plos, and last, but not least, my family and friends, whom I can't thank enough.

Thanks for all your help and encouragement!

Dennis Wiklund

Notations

Roman upper-case letters

A_c	Area of the concrete cross-section
A_s	Cross-sectional area of the reinforcement in the tension zone
A_s'	Cross-sectional area of the reinforcement in the compression zone
A_{sl}	Cross-sectional area of the tensile reinforcement in the section
A_{sw}	Cross-sectional area of the shear reinforcement
$F_{1,1}$	Support reaction in the left support
$F_{1,2}$	Support reaction in the right support
F_{Et}	Tensile force in the longitudinal reinforcement
$F_{Ec,1}$	Compression force in the direction of the support
$F_{Ec,2}$	Compression force in the direction of the inclined strut
F_s'	Steel compression force
G_f	Fracture energy of concrete (model 1)
M_e	Sectional moment
N_e	Axial force in the cross-section due to loading or prestressing
P	Applied point load
S	Section modulus of the cross-section
V	Maximum shear force
$V_{R,c}$	Shear force capacity of the member without shear reinforcement
$V_{R,s}$	Shear force capacity of the member due to shear reinforcement yielding
$V_{R,max}$	Maximum shear force due to crushing of the struts

Roman lower-case letters

a_1	Width of left support strut
a_v	Critical span between the edges of the support and pressure plates
b_w	Smallest width of the cross-section in the tensile area
d	effective depth of tensile reinforcement (loaded from above)
d'	effective depth of compression reinforcement (loaded from above)
f_v	Shear stress
f_b	Bending stress
$f_{b,max}$	Bending capacity of the beam
$f_{v,max}$	Shear capacity of the beam
f_{yw}	Yield strength of the shear reinforcement
s	Spacing of the stirrups
v	Strength reduction factor for concrete cracked in shear
z	Inner lever arm

Greek lower-case letters

α	Angle between strut and main tie
α_{cw}	Coefficient considering the state if the stress in the strut
β	Coefficient of reduction of load due to proximity of load to support
ε_s	Strain of reinforcement in the tensile zone
ε_s'	Strain of reinforcement in the compression zone
σ_{cp}	Concrete compressive stress at the centroidal axis due to loading and/or prestressing
$\sigma_{E,1}$	Stress at support
$\sigma_{E,2}$	Stress in strut
$\sigma_{R,c}$	Maximum stress allowed at the edge of a node in compression nodes
$\sigma_{R,ct}$	Maximum stress allowed at the edge of a node in compression-tension nodes
θ	Angle between the concrete strut and the beam axis

1 INTRODUCTION

1.1 Background

Reinforced concrete deep beams are structural members with a relatively short shear span to their overall sectional depth. They have a wide array of useful applications in building structures, including transfer girders, wall footings, foundation pile caps, floor diaphragms, shear walls, and more. Today, structural engineers have a wide array of different methods available for designing or analyzing the capacity of structural members of reinforced concrete. As sectional analysis is based on beam theory, its applicability to deep beams is questionable. Instead, methods like strut-and-tie modelling (STM) method are available in design codes and can be used relatively easily and cheaply compared to more advanced alternatives. The more complex methods include non-linear finite element analysis (FEA), which attempts to comprehensively model the behavior of the structure. Using the advanced methods is, however, sometimes computationally expensive and often complicated to apply in practice.

1.2 Aim and objectives

The aim of this study was to obtain knowledge regarding the advantages and disadvantages of a number of structural analysis methods in design as well as assessment of the behavior of reinforced concrete deep beams. This covered how these methods vary in suitability and usefulness, including their benefits and limitations, and how they compared in practice in aspects such as accuracy, complexity of calculation, and computation time.

This was achieved by analyzing a number of deep beams previously tested in experiments found in literature. The following analysis and design methods were used and compared in the study: traditional sectional methods, strut-and-tie methods, and non-linear FEA. The main area of application of this study was intended to be as an aid in determining the appropriate methods of design and assessment of reinforced concrete deep beams.

1.3 Limitations

The extent of this study was constrained to three design methods: sectional analysis, STM, and non-linear FEA. All the beams were of reinforced concrete, with ordinary strength concrete and conventional reinforcement steel under different load conditions. Additionally, the beams chosen were limited to those simply supported and with uniform rectangular sections, i.e. with no variance in width or height over the span and no openings and geometric abnormalities, such as notches.

1.4 Method

The method of this study was divided into four steps: literature studies, gathering of experimental data, analyzing reinforced concrete deep beams according to the different analysis methods, and comparing and evaluating the results of the analysis methods against each other and the experimental results. In the literature study, published literature and research papers on the structural analysis methods and their application to reinforced concrete deep beams were reviewed. Experimental results of tests carried out on reinforced concrete deep beams were gathered in parallel to the literature study. Both steps were made by reading and analyzing relevant sources collected from databases like Scopus, Web of Science, and Google Scholar.

The failure load of different reinforced concrete deep beams was determined according to a number of structural analysis methods. The deep beams varied in dimensions, concrete grade, and reinforcement layout. Automated parametric calculations were set up and used to analyze the experimentally tested deep beams with the methods studied. Abaqus was used for FEA and Mathcad was used for manually scripted calculations. In the end, all of the results and observations were analyzed, discussed, and compared to each other to form a comprehensive conclusion.

2 Analysis methods for deep beams

2.1 Discontinuity regions and deep beams

As stated in (Engström, 2015), a discontinuity, or disturbed, region (D-region) is the area of a beam subjected to concentrated loads wherein the concentrated force disperses into a more stable state. This stable state, where plane sections can be assumed to remain plane over deformation and materials have a linear elastic response, defines what is called continuous, or Bernoulli, region (B-region). A deep beam is a beam with a short enough span—when compared to its sectional depth —to make the whole of the member a D-region. This means that, the assumption that plane sections remain plane is likely to be incorrect even in the maximum moment section of a deep beam.

According to Eurocode 2 (EC2) (EN 1992-1-1, 2004) a beam can be considered deep if it has a span that is less than three times its section depth. However, the American Concrete Institute (ACI) (ACI 318-08, 2008) defines deep beams slightly differently. A beam is considered deep if the member is loaded on one face and supported on the opposite face so that compression struts can develop between the loads and the supports, and have clear spans either equal to or less than four times the overall beam's depth. Alternatively, a beam is also considered deep if a concentrated load is applied within twice the depth from the face of the support.

For the purposes of this study, both EC2 and ACI definitions were considered valid descriptions of deep beams. Consequently, a beam was considered deep if the following geometric conditions (for example, see Figure 1) were fulfilled:

$L < 3 \cdot D$ (EC2), $L \leq 4 \cdot D$ (ACI), $s \leq 2 \cdot D$ (ACI).

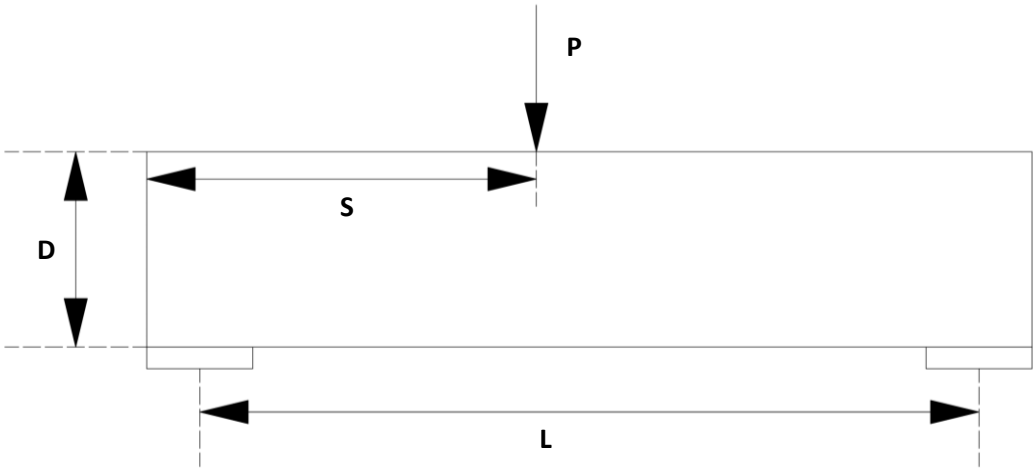

Figure 1 *Geometry of deep beam (example). Adapted from Lecture in Structural concrete 'Design of discontinuity regions' 2017-05-09 by Björn Engström.*

2.2 Sectional analysis method

2.2.1 Description

Sectional analysis methods are traditional ways of evaluating beam action (Al-Emrani *et al. 2011,* Al-Emrani *et. al. 2013*). In these, the geometrical features of the cross-section are described by the area and moment of inertia. The deformations in the cross-section are linked to the displacement and rotation of the beam. The distributed shear and normal stresses acting over the beam's cross section define the inner forces: normal forces (N), shear forces (V), and bending moments (M).

There exist several different beam theories, all with varying assumptions, but all make use of cross-sectional stiffness properties and are based on simplified continuum mechanics. The results are approximations—the efficacy of which depends on factors such as geometry, loads, and boundary conditions—but are often sufficient in practice.

Two of the most commonly used models are Euler-Bernoulli and Timoshenko beam theory. Both theories assume that sections that are plane before deformation remain plane after deformation. Euler-Bernoulli theory, however, also assumes that plane sections remain normal to the neutral axis after deformation while Timoshenko beam theory does not. As a result, the Euler-Bernoulli beam model predicts a bit stiffer response than the Timoshenko model, as it neglects shear deformation of the beam Consequently, the latter is more suited for short span and for thick beams.

2.2.2 Basic design procedure of sectional analysis method

The basic procedure for using sectional analysis method in the design of simply supported beams starts with the construction of a free body diagram. The first step is to compute the sectional forces which the cross-section must withstand, assuming a given design load. With the design load conditions known, it is possible to compute the reaction forces in the supports. Consequently, the bending moment and shear force distribution along the span of the beam can be determined. Of note are the maximum moments and shear forces in the span. There, as well as in other potential locations of interest, a fictitious cut is made through the beam, establishing an imaginary cross-section perpendicular to the beam axis. With this, the internal stresses caused by shear and moment forces are determined for the relevant cross-sections. Based on the loading conditions and dimensions of the cross section, it is possible to determine the maximum internal stresses. The stresses vary over the cross-section.

With stress distribution known, it is a matter of making sure that the load capacity match up, in part by establishing a strength grade of materials—both reinforcement steel and concrete—but also by making sure an appropriate number and size of reinforcement bars that fulfills the required steel area/ratio are present. Both shear and bending needs to be looked at.

In other words, the following checks should be made:

$f_{b,max} > f_b, \quad f_{v,max} > f_v$

$f_{b,max}$ = bending capacity, $\quad f_{v,max}$ = shear capacity,

If the serviceability limit state (SLS) is relevant, the requirements regarding deflection and crack width should also be accounted for. However, if only the ultimate limit state (ULS) is of concern, then investigating these parameters are not necessary.

2.3 Strut-and-tie method

2.3.1 Description

The strut-and-tie modelling (STM) method is a design method based on the theory of plasticity that makes use of a theoretical truss-system to mimic the stress field in cracked reinforced concrete members (Engström, 2015). This is done by simulating the flow of forces in the structural member, after plastic redistribution, with a sequence of struts, ties, and nodes linking the two together. The struts and ties represent flow of compressive and tensile stresses, respectively. The first is typically carried by concrete and the latter by reinforcement. For a visual example of what this might look like, see Figure 2. The method is applicable only to the ULS and not the SLS

The strut-and-tie method is a lower bound plastic theory approach. This means that it is reliable if equilibrium towards external load is satisfied, the ductility is adequate against redistribution of forces, and the struts and ties are formed in such a way as to properly resist the design forces. Important to note is that the theoretical failure load achieved by this method is lower than the actual failure load, which means that, though the solution is not necessarily the most efficient, it is considered safe to use even in atypical situations, like in discontinuity regions.

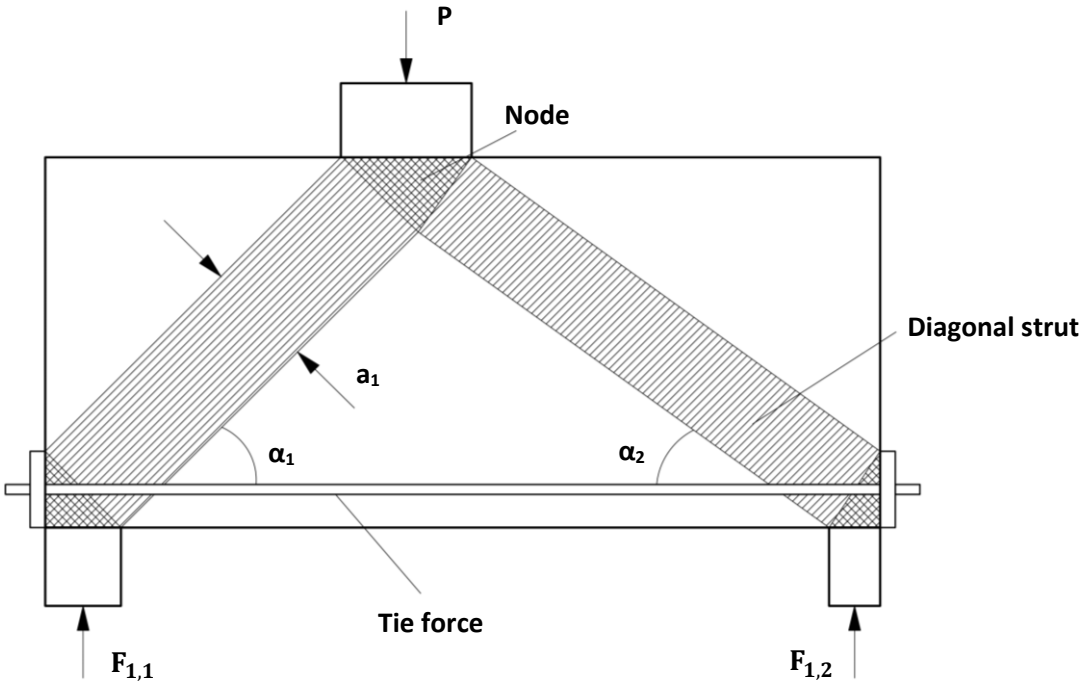

Figure 2 *Example of strut-and-tie model of a deep beam under a three-point load. Adapted from ACI Section 10.7.1 For Deep Beam.*

There are, however, some challenges common to the STM method (Panjehpour *et al.*, 2012). One of these are that using the method to analyze a given member achieves different results depending on the design codes or standards used. Another is that strain compatibility does not need to be satisfied in STM. This means that there is no unique STM solution for any given member analyzed and that empirical engineering judgement may need to be applied. Finally, depending on the way the member forces are provided, the STMs can be allocated either statically determinate or indeterminate to the static uncertainties of STM.

2.3.2 Basic design procedure of strut-and-tie method

The process of the STM design method is commonly (Sam-Young, Chang-Yong and Kyeong-Min, 2007; Engström, 2015) described as a general outline consisting of several steps. The first step is to perform a basic structural analysis. This entails defining the structural system, identifying support reactions and sectional forces under design load, as well estimating the sizes and proportions of the beam member.

The next step consists of defining the beam's continuity (B-) and discontinuity (D-) regions. The D-region areas can generally be found using model codes, based on the elements' geometry and loading conditions. Then, the stress distribution between the two regions is ascertained and the B-region designed according to methods other than the STM method. Consequently, the D-region is analyzed to form a reasonable stress field and a strut-and-tie model is constructed either according to the load-path method or from principal stresses and stress trajectories found by linear FEA.

Finally, the forces in the components of the strut-and-tie model is found using equilibrium. The ties are designed and the nodes and struts are verified with respect to the stress capacity. If needed, the dimensions of the components of the strut-and-tie model are iterated and optimized to not over-stress the components. Figure 3 illustrates the design modelling steps as a flow chart.

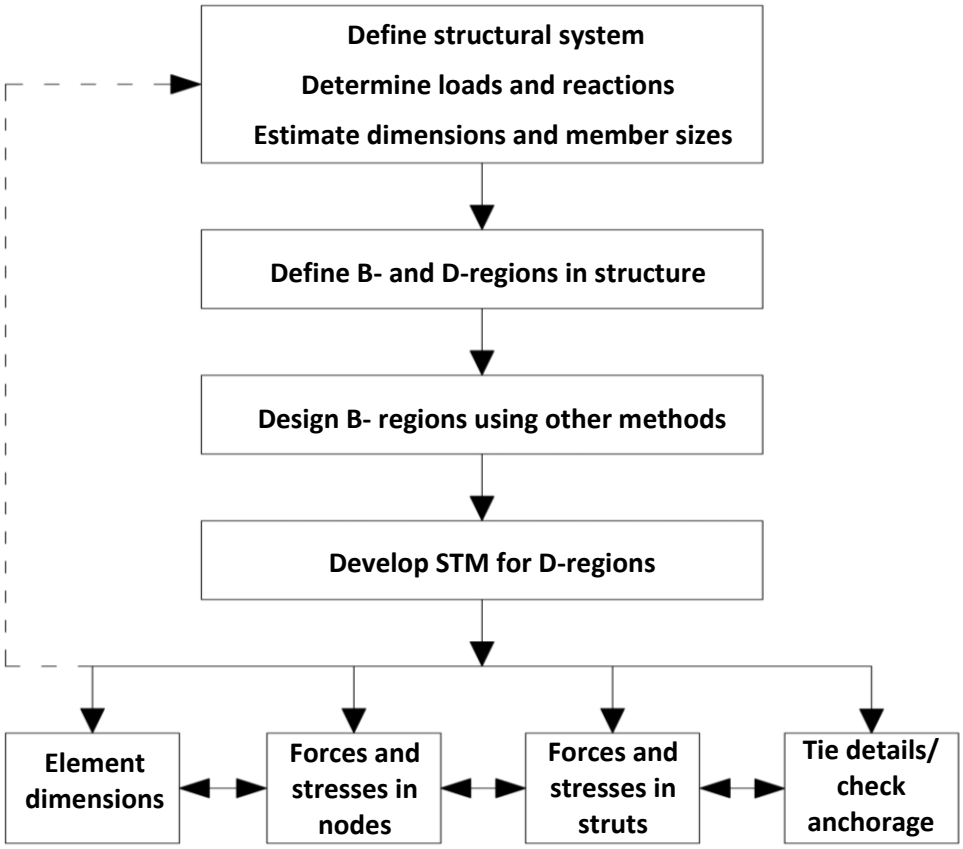

Figure 3 *STM model design flow. Adapted from 'The strut-and-tie model of concrete structures' 2001-08-21 by Dr C. C. Fu.*

2.4 Non-linear finite element analysis

2.4.1 Description

The finite element method (FEM) is a method of finding an approximate solution to a partial differential equation. It is a suitable method for the modelling of structures with non-conventional shapes or under conditions where the effects of multi-directional states of stresses are of concern (Mario Plos, 1996). In many circumstances, it is satisfactory to assume linear elastic material behavior, which results in a linear system of equations to solve. Contrarily, under circumstances where the nonlinear behavior is of concern, a non-linear method can be employed.

Typically, modest loads are enough to cause cracking in concrete structures and, even as early as in the SLS, the non-linear material behavior initiated by the cracking manifests. Thus, linear solutions are of limited use when it comes to analyzing the response of concrete structures. In the ULS, once crushing in the concrete in the compressive zones and yielding in the reinforcement bars in the tensile zones have initiated, the use of linear material response as a premise for the material model runs the risk of obtaining entirely misleading results. Under such circumstances, non-linear analysis should be used to construct a more accurate representation of the material behavior.

With the ever-increasing role of software using FEA for modelling of reinforced concrete structures, it becomes more and more important for the engineers of tomorrow to possess at least a rudimentary understanding of the analysis methods based on finite elements. Non-linear FEA requires the analyst to make a multitude of decisions concerning the degree of detailing appropriate for the modeling of a structural problem. Such decisions include, among others, what material models, structural solution methods, and type of finite elements to use and the choices made are vital for how close the model comes to accurately mimic the real response of the structure. It is important to show the decision-making, not just for the analyst but also for everyone who will use the results of the analysis for their own work, so that they may assess its quality for themselves.

A common challenge for the FEM is its application to civil engineering structures, due to the large structure size, complex connections, the variety of parameters, etc. Thus, methods to update the FEM for such cases have been developed, like the direct algorithm, iterative algorithm, and intelligent optimization (Wang *et al.,* 2013). The typical way of solving non-linear finite element problems is through incremental iterative solution methods (Kong, 2002). For modeling of concrete structures, three-dimensional non-linear material models are most often chosen for both the concrete and the reinforcement.

2.4.2 Basic analysis procedure of non-linear finite element analysis

The FEA of complex structures is usually performed using computer aid, typically in the form of a FEA-based simulation program. The exact computation differs slightly between softwares, but the general procedure follows three steps:

1. Preprocessing: in this step, the data and input needed to properly simulate the behavior of the user-made model is given. This includes the meshing—segregating the model into several sub-regions, called elements, linked through discrete nodes—as well as the material properties and boundary conditions, either in load or displacement, applied to specific nodes. For an example using the software Abaqus, see Figure 4.

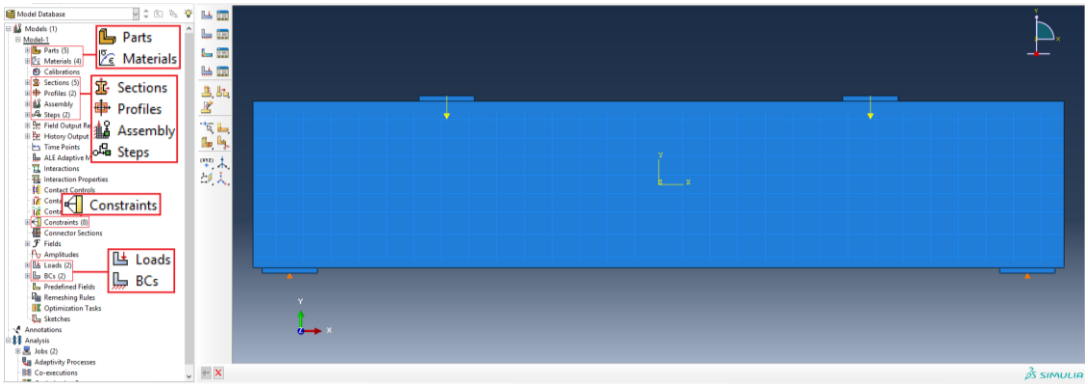

Figure 4 *An example of pre-processing in Abaqus, with some important parameters highlighted.*

2. Solution/analysis: this step entails submitting the model to the solver as input for finite element code. The code solves a sequence of linear or non-linear equations to produce a result of numerical outputs of displacement, stress, etc. in the nodes.

3. Postprocessing: the postprocessing step provides a visual aid—colored contours or gradients, for instance—to showcase the results to the user in a more readable way. For an Abaqus example, see Figure 5.

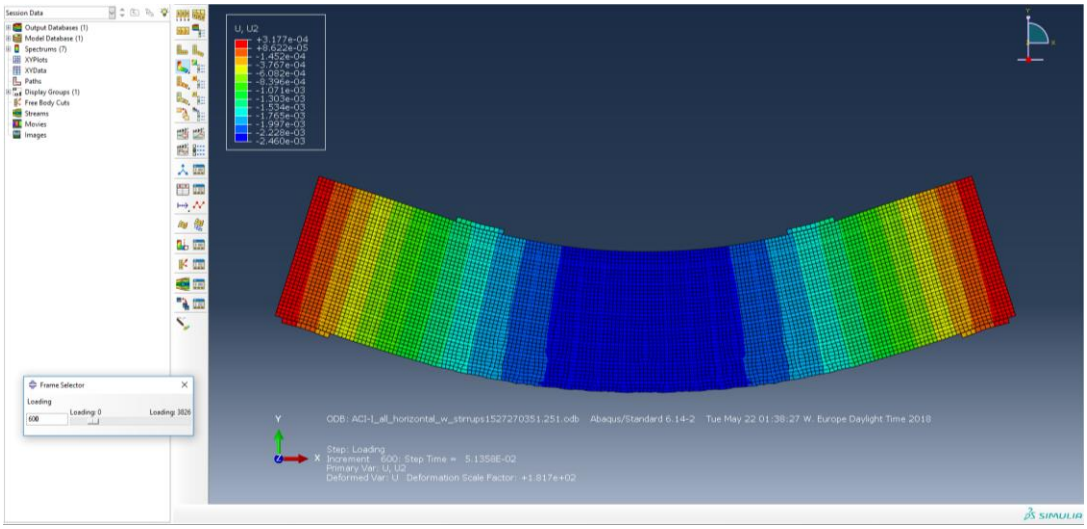

Figure 5 *An example of post-processing in Abaqus, studying the beam's deformation in the y-direction.*

3 Analysis of tested deep beams

3.1 Collection of experimental data

The collection of experimental data was performed by searching for papers detailing loading tests conducted on reinforced concrete deep beams. The data of interest included deep beam geometry, concrete grade, reinforcement strength and layout, applied load, etc. Relevant sources were found by searching for key-words—like 'deep beams', 'reinforced concrete', 'simply supported', 'strut-and-tie method', or 'finite element modeling', etc. The level of relevance of the generated hits were confirmed by examining the abstracts, tables of contents, and summaries. The more important sources were then read more thoroughly to discern the more significant pieces of information.

The filtered sources were subsequently reviewed and categorized based on several factors. For example, the sort of load the deep beams were subjected to, concentrated or distributed load, or the length-to-height ratio, low or very low. Then, the reinforcement layout, especially the presence (or lack) of shear reinforcement, was considered. Primary sources—those that described the procedure of their own tests instead of referencing another's—were also prioritized. Finally, the information was extracted and used to model the behavior of the reinforced concrete deep beams using sectional analysis, STM, and non-linear FEA methods.

Six deep beams were analyzed in this study. Of these, two beams (called ACI-I and STM-M, respectively (Abdelrahman, Tadros and Rizkalla, 2003)) were variations of each other, as were two other beams (called A1 and A3 (Quintero-Febres, Parra-Montesinos and Wight, 2006)**).** All the beams had geometry well within the limits for deep beams (see Section 2.1) and five of them had a height significantly (at least a third) smaller than the total length. All beams, including their reinforcement layout, can be seen in Figures 6-11 and, in even more detail, in Appendix A.

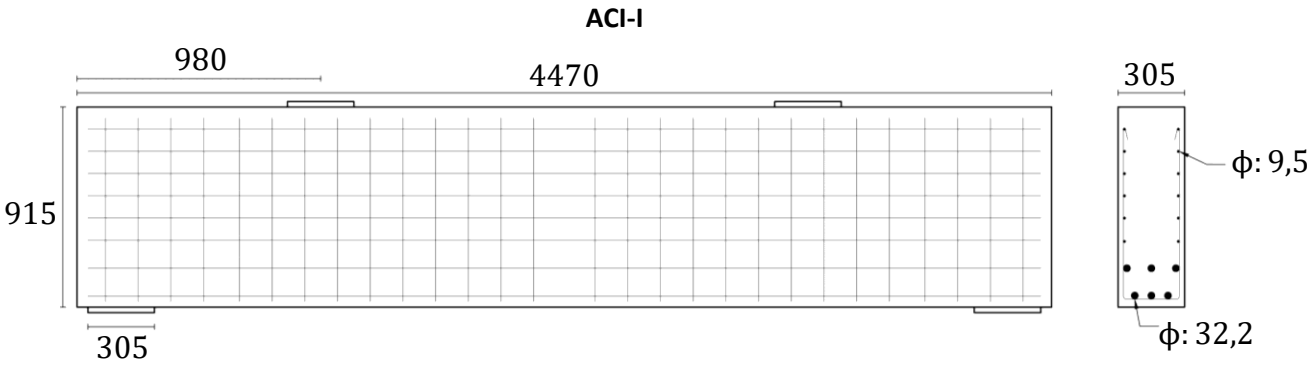

Figure 6 *A sidewise view and section in critical shear span of beam ACI-I. The vertical rebars are 9,5 mm in diameter. Adapted from (Abdelrahman, Tadros and Rizkalla, 2003).*

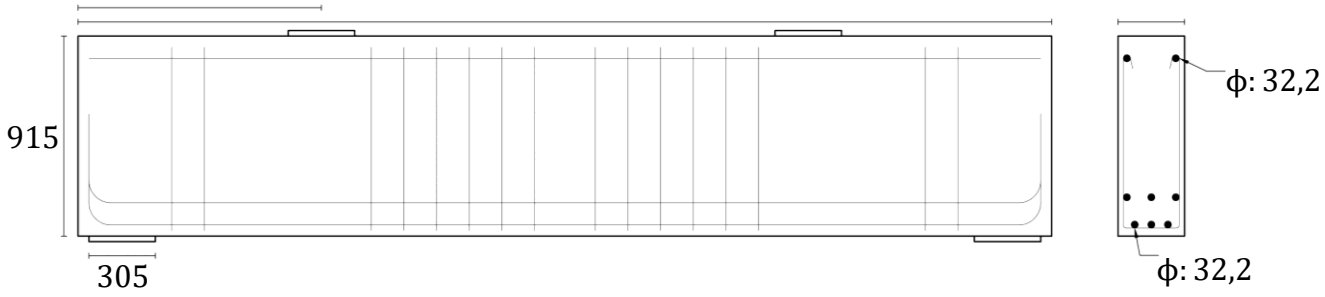

Figure 7 *A sidewise view and section in critical shear span of beam STM-M. The vertical rebars are 9,5 mm in diameter. Adapted from (Abdelrahman, Tadros and Rizkalla, 2003).*

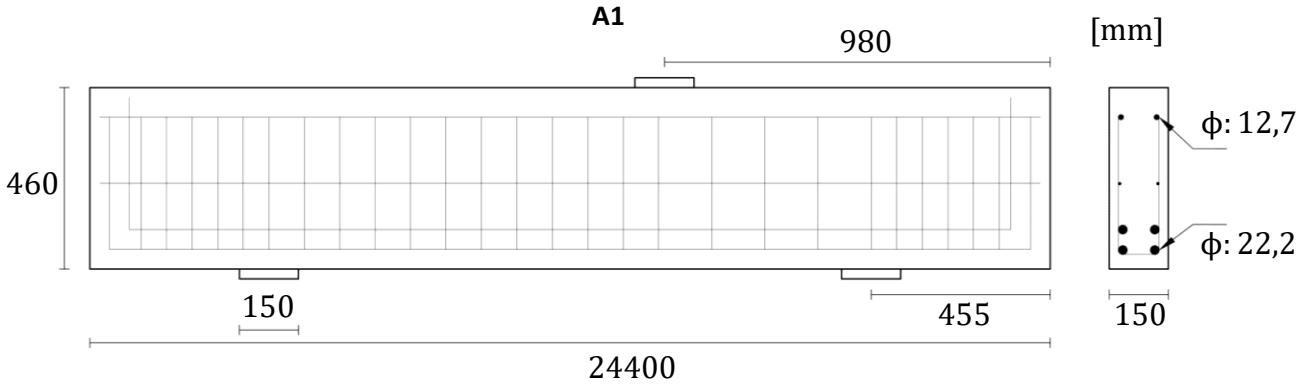

Figure 8 *A sidewise view and section in critical shear span of beam A1. The vertical rebars are 6,4 mm in diameter. Adapted from (Quintero-Febres, Parra-Montesinos and Wight, 2006).*

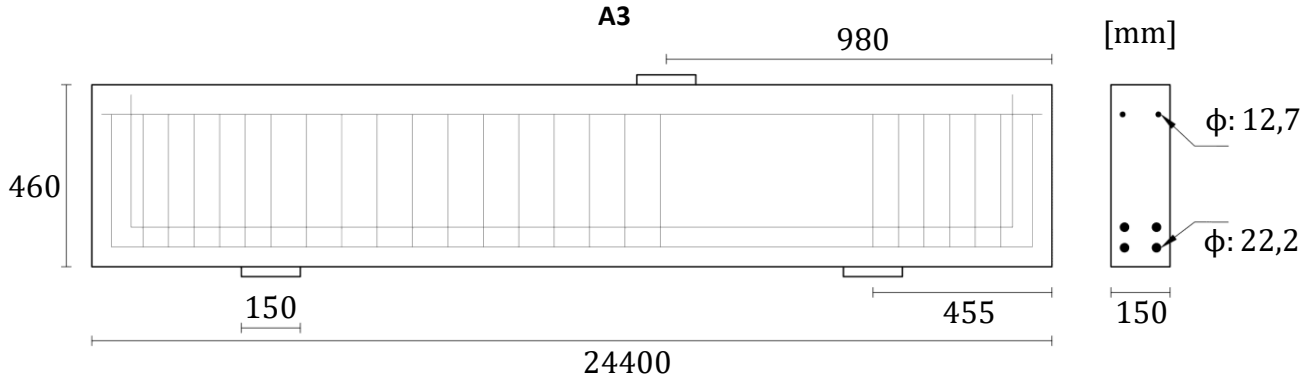

Figure 9 *A sidewise view and section in critical shear span of beam A3. Adapted from (Quintero-Febres, Parra-Montesinos and Wight, 2006).*

In the BS-355 beam (Birgisson, 2011) the support reactions and pressure loads were applied through cylindrical rollers directly, without the typical support and pressure plates in between. This made the applied pressure loads and support reactions act more concentrated, on a small concrete surface. In the last beam, the "L&W" (for Leonhardt and Walther) beam (Vecchio, 1989), the length-to-height ratio was much lower than the already low ratio of the other beams, with equal size for the length and height of the beam.

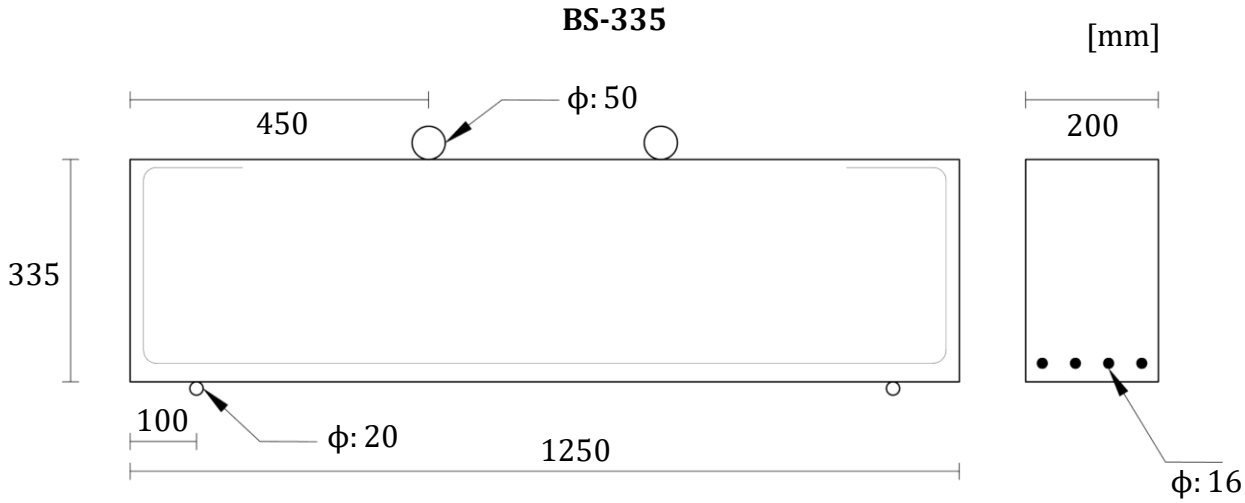

Figure 10 *A sidewise view and section in critical shear span of beam BS-355. Adapted from (Birgisson, 2011).*

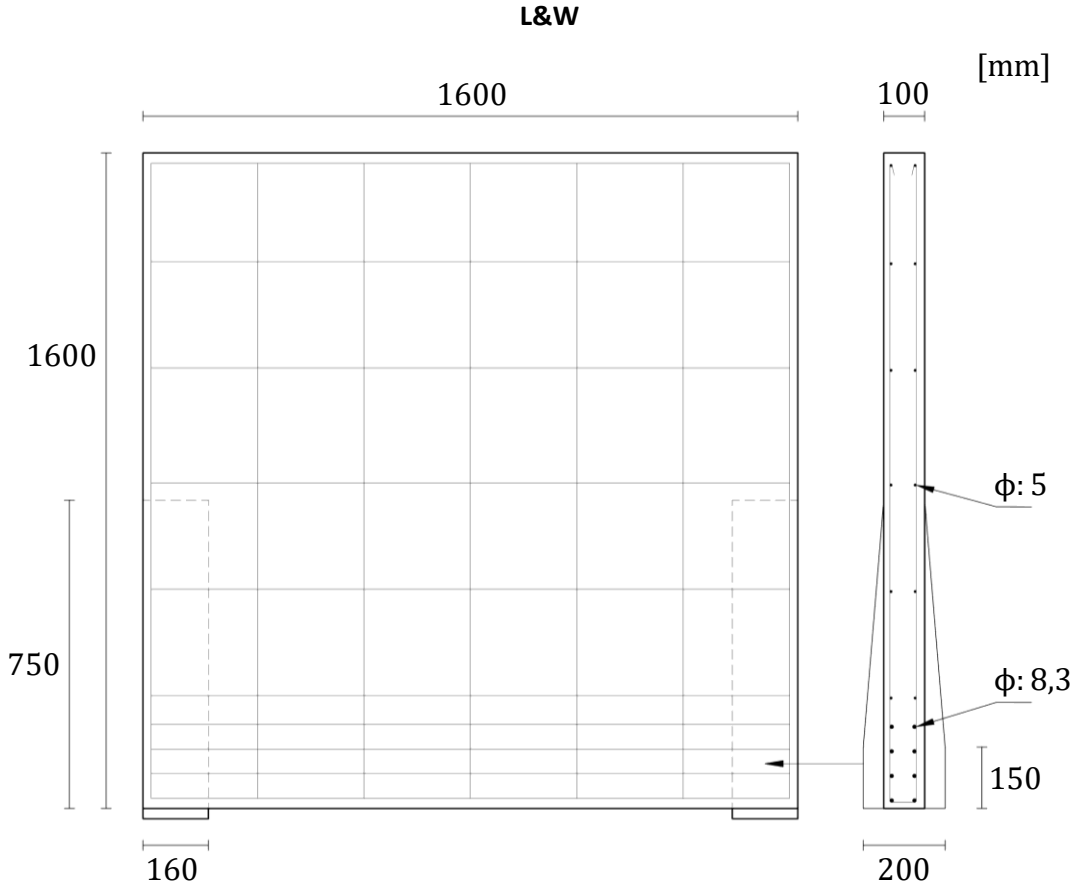

Figure 11 *A sidewise view and section in critical shear span of beam ACI-I. The vertical rebars are 5 mm in diameter. Adapted from (Vecchio, 1989).*

The beams also differed in their method of load application. Specifically, the ACI-I, STM-M, A1, A3, and BS-355 beams were subjected to point-loads. The L&W beam, however, was subjected to a distributed load. Beam ACI-I, STM-M, and BS-355 were loaded symmetrically by two-point loads (four-point bending) while beam A1 and A3 were loaded symmetrically by one-point load (three-point bending). For a more detailed description, see Appendix A.

In addition, the beams' material properties, particularly the strength of the concrete and reinforcement steel, were gathered from the experiment references and used in the structural analyses. The material strengths can be seen in Table 1 below.

BEAM	$f_{y,main}$ (MPa)	$f_{y,shear}$ (MPa)	$f_{y,secondary}$ (MPa)	$f_{concrete}$ (MPa)
BS-335	530 (measured)	-	-	31,43 (measured)
L&W	415	415	415	29,6
STM-M	420 (measured)	450 (measured)	450 (measured)	28 (measured)
ACI-I	420 (measured)	450 (measured)	450 (measured)	33 (measured)
A1	462 (assumed)	407 (assumed)	455 (assumed)	22 (measured)
A3	462 (assumed)	-	455 (assumed)	22 (measured)

Table 1 *Yield and mean compressive strengths for the reinforcement steel and concrete, respectively, of each beam, extracted from their respective experiment references. The values designated '(assumed)' assumed standard values based on grade of material ordered. Conversely, the values designated '(measured)' are based on tests conducted as part of the experiment reference's investigations. For the undesignated values, the experiment reference did not specify if they were measured or assumed.*

3.2 Structural analysis

3.2.1 General

To gain as accurate load capacities as possible, the mean concrete strength (or concrete strength given in the reference for the experiment) was used instead of design concrete strength. This held true for all the analysis methods, both to improve the measure of accuracy but also to make sure that the comparisons of results were authentic.

3.2.2 Sectional analysis

The load capacity according to sectional analysis was identified mainly by applying calculations based on design methods from EC2 and (Al-Emrani *et al. 2011,* Al-Emrani *et. al. 2013*) to Mathcad script. Sectional analysis was used to investigate resistance with respect to two failure modes, bending and shear. The shear resistance was checked according to four different failure criteria.

Firstly, the load capacity with respect to bending was determined. The code in the main Mathcad file was set up to automatically calculate the bending capacity for each deep beam, only including the concrete cross-section and tensile reinforcement bars. Some of the deep beams, however, had secondary layers of reinforcement outside of the main tensile reinforcement. For those, the initial results from the main Mathcad file served only to give a preliminary bending capacity. To find the full bending capacity of these deep beams, additional Mathcad files were written for each of them separately to take into account their secondary layers of reinforcement.

Next, the load capacity according to shear resistance was calculated in Mathcad using the methods outlined in EC2. There were several failure criteria for shear that had to be checked for each deep beam: maximum shear force limited by the crushing of the inclined web compression struts (web shear compression failure), shear force which can be sustained by the yielding shear reinforcement, and shear resistance of the member without shear reinforcement. For web shear compression failure, different criteria according to EC2 was used depending on if the beam had shear reinforcement in its critical span or not.

When calculating shear capacity with respect to yielding of shear reinforcement ($V_{R,s}$), the number of stirrups in the critical shear span ($\frac{A_{sw}}{s} \cdot z$) was already known and given directly. For members with load applied on the upper side of the beam within a distance $0{,}5 \cdot d \leq a_v \leq 2{,}0 \cdot d$ from the support, the contribution of this load to the shear force V_E was reduced by $\beta = a_v / 2 \cdot d$.

The shear force V_E, calculated in this way checked to satisfy the condition $V_E \leq A_{sw} \cdot f_{ywd}$, where $A_{sw} \cdot f_{ywd}$ is the resistance of the shear reinforcement crossing the inclined shear crack between the load and the support (see Figure 12).

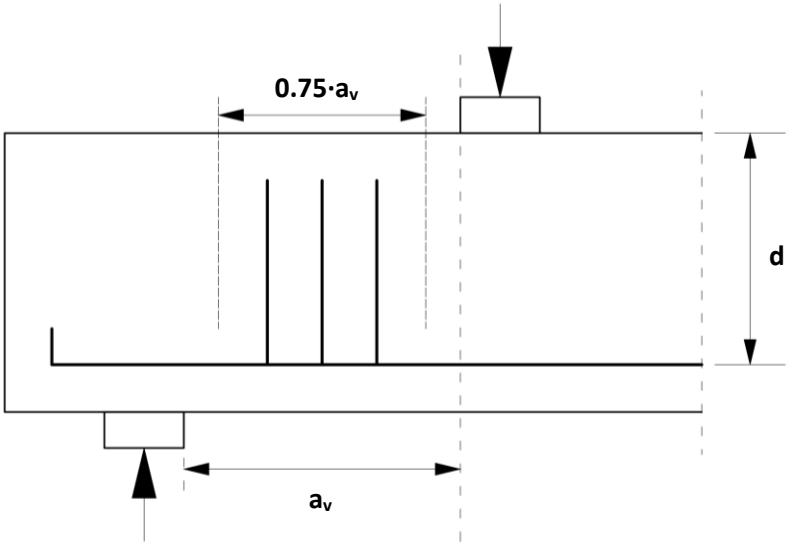

Figure 12 Beam with load near direct support. Adapted from EC2 Section 6.2 'Shear'.

Only the shear reinforcement within the central $0{,}75 \cdot a_v$ was included. The longitudinal reinforcement was assumed to be fully anchored at the support.

3.2.3 Strut-and-tie analysis

According to standard STM design procedure, the load in the deep beam with distributed load conditions were simplified into equivalent concentrated loads in order to determine a viable load path.

Before the calculations were conducted, the data needed for the analyses—found in the experiment references—were collected in an Excel file. The contents of the Excel file were then used as a source of input of data for the Mathcad script used to calculate the ultimate load capacity according to STM methods. The Mathcad script was linked to the Excel file in such a way that with the change of just one variable in Mathcad, the data of one beam or another was called upon. The analysis was performed a bit differently depending on which of several categories the deep beams belong to (distributed vs. concentrated loads, symmetrical vs. asymmetrical loading, etc.).

With the proper input data, a strut-and-tie model was rendered in accordance with EC2. The optimal angle of the inclined strut was found by iteratively lowering the maximum angle between the tie and the compression strut at the support until the requirements for strut compression capacities were fulfilled. Based on the relationships defined by this angle and the yield capacity of the reinforcement in the tie, the equilibrium in the critical nodes could be established. From that, the load capacity according to strut-and-tie model was determined.

Analysis calculations
The relationships used in the calculations and analyses were based on the section ‘6.5 Design with strut and tie models’ in EC2. First, the maximum allowable stresses for compression and compression-tension nodes were established. Concurrently, a preliminary strut angle α was determined, i.e. the angle between the concrete compression strut and the tensile force in the tie, the longitudinal reinforcement, see Figure 13. This preliminary angle was used as an input value to a for-loop in the Mathcad code. The preliminary strut angle was then successively lowered slightly for each increment and the stresses of both nodes and struts were determined. This was made keeping equilibrium and assuming yielding in the tensile reinforcement bars. The for-loop delivered the maximum allowed strut angle for which the concrete strength was not exceeded.

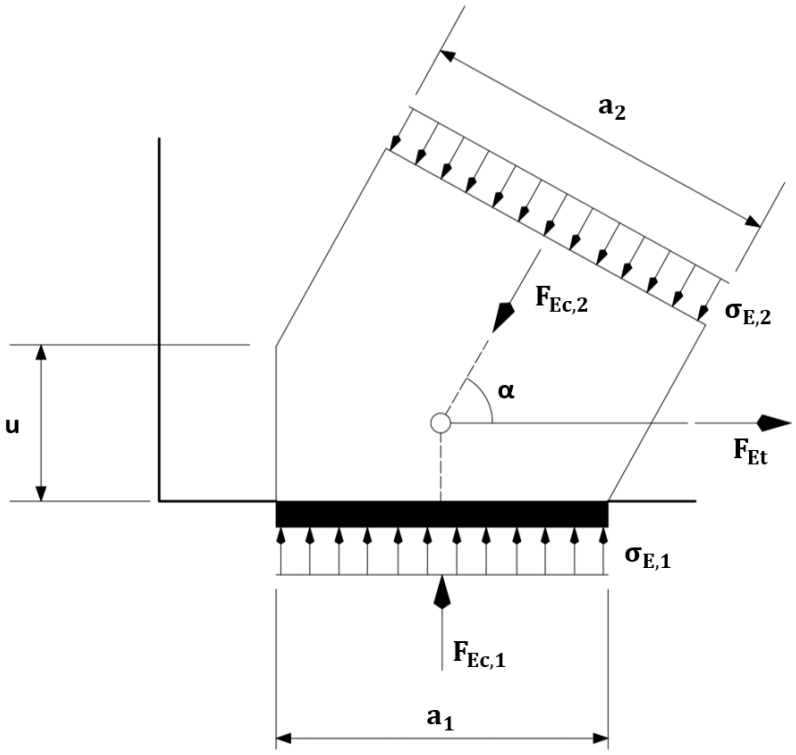

Figure 13 *Compression tension mode with reinforcement provided in one direction. Adapted from EC2 Section 6.5 'Design with strut and tie models'.*

With the strut angle known, it was possible to generate an image of the STM model in Mathcad (for an example, see Figure 14). Finally, a set of equilibrium equations were constructed based on the strut angle and the yielding capacity of the tensile reinforcement bars to determine all stresses and forces in the STM model together with the applied load. This was the load capacity according to the STM method. According to EC2, the compressive stress could also be increased by 10% when the strut angle was $\alpha \geq 55°$.

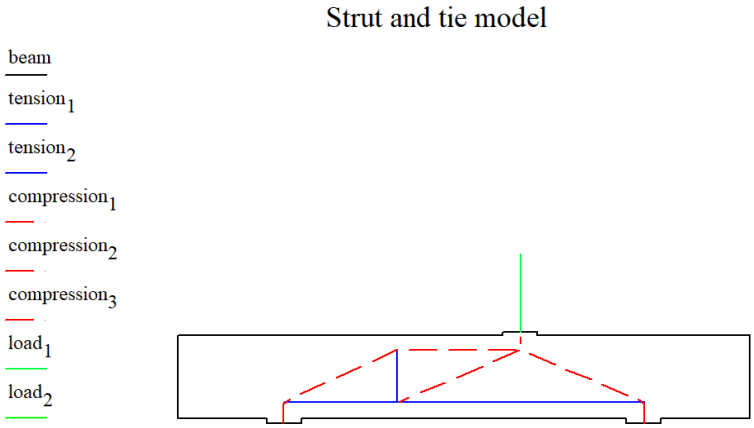

Figure 14 *ST model of beam A3 constructed in Mathcad*

3.2.4 Non-linear finite element analysis method

The non-linear FE analyses were performed using the program Abaqus CAE. For this study, Abaqus version 6.14-2 was used. The computations were performed in resources at the Chalmers Centre for Computational Science and Engineering (C3SE) provided by the Swedish National Infrastructure for Computing (SNIC).

Abaqus is a computer modeling software based on FEA dating back to 1978, made to handle non-linear physical behaviors. The program makes use of the scripting and coding language Python, which was used during the study to set up beam test models. For a more detailed recollection of all input values, see Appendix A.

Due to the thickness out of plane being relatively small, the deep beams were modeled in Abaqus as 2D models, in accordance with Figures 6-11, and with the assumption of plane stress/strain. The sections of the main beam parts were set as a solid homogenous type, with concrete material assigned and a thickness depending on the deep beam being analyzed. The materials have been modeled according to non-linear material models that describe the cracking of the concrete and the plastic behavior of the reinforcement. Also, the reinforcement has been modeled assuming a perfect bonding to the concrete.

Geometry
With a 2D analysis, it was important to properly model the sections of each part. For the analysis of any one deep beam, the section of the main beam part was simple and constant throughout its span, but the reinforcement sections were potentially more varied. They could differ between horizontal and vertical, or between tension and compression, or even within these categories (see Section 3.1). It was also important to account for the number of bars in each line of reinforcement. The vertical lines were always composed of two stirrups per line, but the number of reinforcement bars in each horizontal line could vary. This affected the cross-sectional area assigned to the reinforcement lines. Since the lines represented multiple reinforcement bars, the contribution of all the bars to the cross-sectional area had to be included. A circular profile was constructed for each different variety of reinforcement lines, with a defined radius that corresponds to the total area of all the bars in the line.

Boundary conditions and loads
The deep beams were modeled as simply supported, typically resting on support plates positioned at each end of the beams. The node in the center of both support plates' bottom edge was locked in the vertical direction and one of them in the horizontal. The way of modeling the load varied slightly between the different deep beam analyses. In the case of distributed load, the load was applied directly on the top of the beam. With concentrated loads, the load was applied on a pressure plate distributing the force. These plates had the same material parameters as the support plates and were tied to the main body of the beam in the same way. Since the intention was to study the behavior up to the maximum load only, the analyses were made with load control and displacement control was not used.

Materials
The material properties for the models were, when available, based on the references from the experiment of each deep beam studied. When a value for a parameter was not given, a standard value was used or an estimate was made.

A mass density of 2400 kg/m^3 was assumed for concrete. The concrete's elastic properties, specifically Young's modulus and Poisson's ratio, were assumed to be 33 GPa and 0.2, respectively, for all the beams.

To model the non-linear behavior of concrete, the Concrete Damage Plasticity (CDP) model was used. The input parameters of CDP are grouped into compression, tension, and plasticity parameters. The compression parameters were the compression yield stress and the inelastic strain. The compression yield stress for an inelastic strain of zero was set to the mean strength (see Table 1). The stress for an inelastic strain of 1 was either the ultimate strength, when provided by the source, or the concrete was assumed to be perfectly plastic. This means that compression failure is not fully simulated in the analyses, but that the concrete acts according to plastic behavior, which is reasonable for the purposes of this study.

The tensile parameters were tensile yield stress and fracture energy. The tensile yield stress was specified to the mean tensile strength according to the experiments but, if unspecified, assumed to be 5 MPa. The fracture energy was calculated based on the mean compressive strength of the in accordance with Model Code 2010 (fib, 2013):

$$G_f = 73 \cdot {f_{cm}}^{0.18}.$$

The plasticity parameters are the dilation angle (in the p-q plane), the flow potential eccentricity, the ratio of initial to biaxial compressive yield stress (fb0/fc0), the K-ratio, and, optionally, the viscosity factor. For the analyses in this study, the dilation angle, the flow potential eccentricity, fb0/fc0, and K were assumed to be, in accordance with recommended default values in Abaqus, 35°, 0.1, 1.16, and 0.67, respectively. The viscosity factor was set to 1e-7 based on parametric studies.

The steel material used in the analyses were different for reinforcement and plates (pressure and support). Depending on the deep beam being analyzed, the reinforcement could be divided into different sets depending on, among other things, the reinforcement bars' strength grade. The mass density of the steel was assumed to be 7850 kg/m^3, Poisson's ratio was assumed to be 0.3. The reinforcement steel's Young's modulus was assumed to be 200 GPa. However, for the loading plates it was assumed to be a thousand times larger than the real Young's modulus to give the support and pressure plates a very large stiffness and allow them to rotate around their center while remaining rigid. Finally, the yield stress specified in the experiment reference was assigned to the reinforcement steel. For an inelastic strain of zero, the mean yield stress was applied (see Table 1). For an inelastic strain of 0.048, the yield stress was set either to the ultimate strength, when provided by the source, or the steel was assumed to be perfectly plastic.

Interaction between concrete and reinforcement:
For this study, the concrete-to-reinforcement interaction was modeled assuming perfect bond using embedment connection. The reasoning behind this was two-fold. Firstly, for this study, it was enough to simulate the general response of the deep beams even if the cracking is not reflected in detail. Also, it was because embedment typically falls between discrete and distributed in terms of complexity and ease of implementation (Li, 2007).

Elements
The type of elements used in the analysis varied between the different parts of the model. The main concrete part of the beam was composed of plane stress elements. The concrete parts of the high beams were modeled using 4-node bilinear plane stress elements, denoted CPS4R in Abaqus. The type of finite elements for the reinforcement differed between the horizontal compression and tensile reinforcement bars, and the vertical shear reinforcement. The horizontal reinforcement was modeled using linear 2-node beam elements, denoted B21, and the vertical reinforcement was modeled using linear 2-node truss elements, denoted T2D2. The total number of elements varied between the different beam analyses (see Appendix A). A mesh convergence study was made for each beam model to make sure a sufficiently fine element mesh was used.

Solution method:
The static FE-analysis was made using the general procedure type in Abaqus, assuming no non-linear geometry effects. No automatic stabilization was applied. An automatic incrementation procedure was used, with a minimum increment size of 1e-9 and both the initial and maximum increment sizes set to 0.1. The analyses were set to use a direct equation solver to solve linear systems of equations and a Full Newton solution technique to solve non-linear systems of equations iteratively by linearizing them. The analysis was set to stop either when a step had reached the maximum number of increments, 1000000, or the increment size had decreased to less than the minimum increment size, 1e-9. To assure that beam failure had been found and that the analysis had not stopped just because of convergence failure, the model's behavior, like the load-displacement behavior, was compared to those of the experimental references'.

Once done, the results were converted from numerical outputs into visual information accessed in Abaqus's visualization module. From there, the results could easily be read visually at a glance. For example, principal strains were observed directly in the module to study the propagation behavior of cracking over time. Finally, the load-displacement curves of the simulation were extracted from the module and exported to an Excel file sheet, where they could easily be compared with the load-displacement curves derived from the experiment references.

4 Results

In this section, the results are shown for sectional analysis, STM, and non-linear FEA. For all the methods, the load capacities according to the analyses and the experiment tests are compared visually in a bar chart and numerically in a table. For the non-linear FEA method, the results also include the load-displacement curves.

Important to note is that that the results in Figures 15-17 and Tables 2-4 differ from the maximum load in most of the curves in Figures 18-23, showing the load-displacement relationship. This is because the first set of figures and tables show the total load. Meaning that, in the case of distributed load, it measures the load over the whole load distribution and in the case of four-point loading, it considers both applied load, etc. Figures 18-23, meanwhile, differ in ways of measurement depending on how the source presented them. This was to allow for a better comparison between the load-displacement curves from Abaqus and the test experiments.

4.1 Sectional analysis results

The results of the sectional analysis include the capacity with respect to both bending and shear. For the load capacity according to bending and shear, see Figures 15 and Table 2.

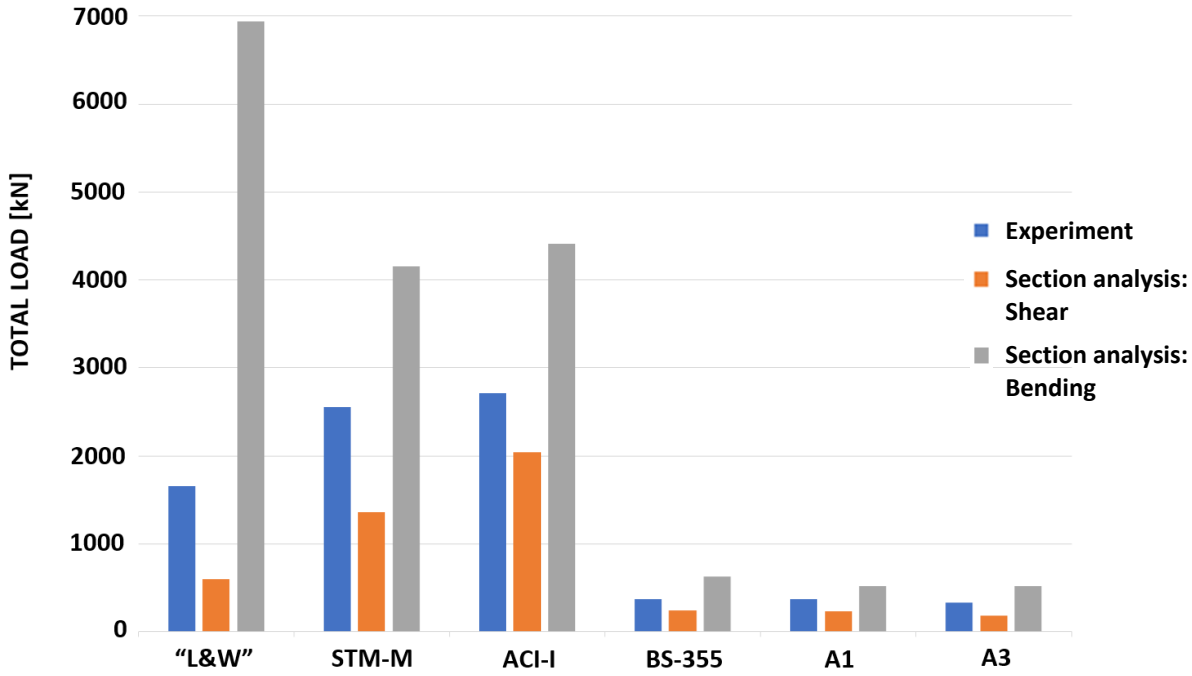

Figure 15 Load capacity according to sectional analysis

	Deep beam					
	L&W	STM-M	ACI-I	BS-355	A1	A3
Exp. capacity [kN]	1650	2550	2700	375	375	330
Bending capacity [kN]	6940	4150	4410	635	525	525
Ratio (Bending/Exp.)	4.2	1.63	1.63	1.69	1.4	1.6
Shear capacity [kN]	600	1360	2040	250	230	180
Ratio (Shear/Exp.)	0.36	0.53	0.76	0.67	0.61	0.55

Table 2 *Load capacity according to sectional analysis, with respect to bending and shear, respectively, compared to experiment failure loads.*

During the study, shear capacity with respect to web shear compression, compression crushing, and shear capacity without or with shear reinforcement, respectively, were investigated. The shear capacity shown here is the maximum capacity with respect to the different possible failure modes.

4.2 Strut-and-tie results

The maximum total load according to FEA, compared to the total experimental maximum load, can be seen visually in Figure 16 and numerically in Table 3.

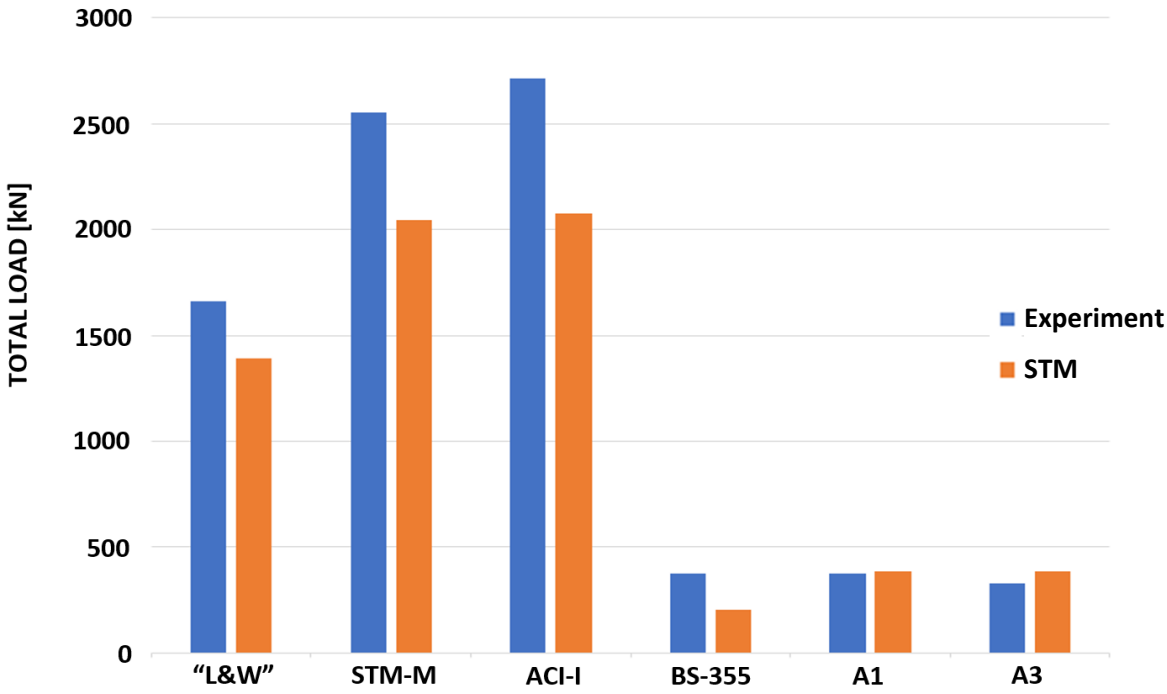

Figure 16 *Load capacity according to STM method*

	Deep beam					
	L&W	STM-M	ACI-I	BS-355	A1	A3
Exp. capacity [kN]	1650	2550	2700	375	375	330
STM capacity [kN]	1390	2050	2080	205	385	385
Ratio (STM/Exp.)	0.84	0.8	0.77	0.55	1.02	1.17

Table 3 *Numerical results of load capacity according to STM*

4.3 Non-linear finite element analysis results

The maximum total load according to STM, compared to the total experimental maximum load, can be seen in Figure 17 and numerically in Table 4.

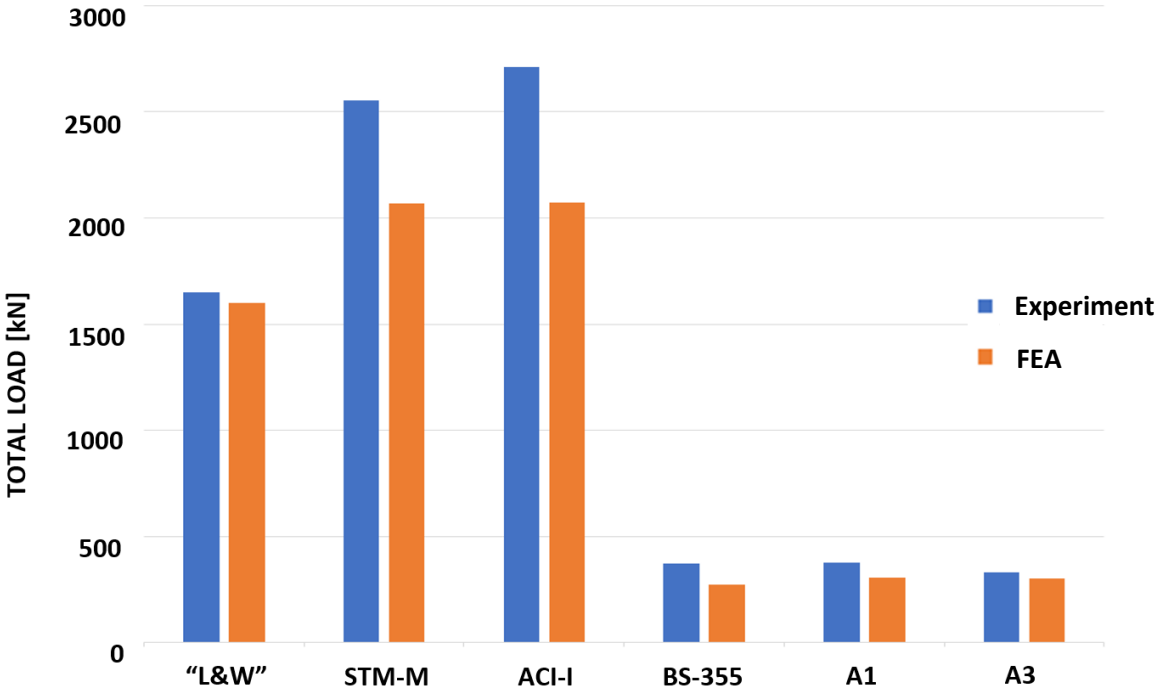

Figure 17 *Load capacity according to Abaqus based on FEA method*

The load-displacement curves of the various deep beams can also be seen in Figures 18-23. Important to note is that the load-displacement curves from the sources' test experiments were sometimes altered, due to some misleading measuring of displacement. For example, the curves would often start with a very quick increase in deformation with little or no accompanying load measured. This was probably because the movement of the machine was measured. To make for a more accurate comparison with the load-displacement curves from the Abaqus analyses, the test experiments' curves were moved to start where a sizable increase in load was registered.

Non-linear FEA

	Deep beam					
	L&W	STM-M	ACI-I	BS-355	A1	A3
Exp. capacity [kN]	1650	2550	2700	375	375	330
FEA capacity [kN]	1600	2070	2070	275	305	305
Ratio (FEA/Exp.)	0.97	0.81	0.77	0.73	0.81	0.92

Table 4 *Numerical results of load capacity according to Abaqus*

4.3.1 Load-displacement charts

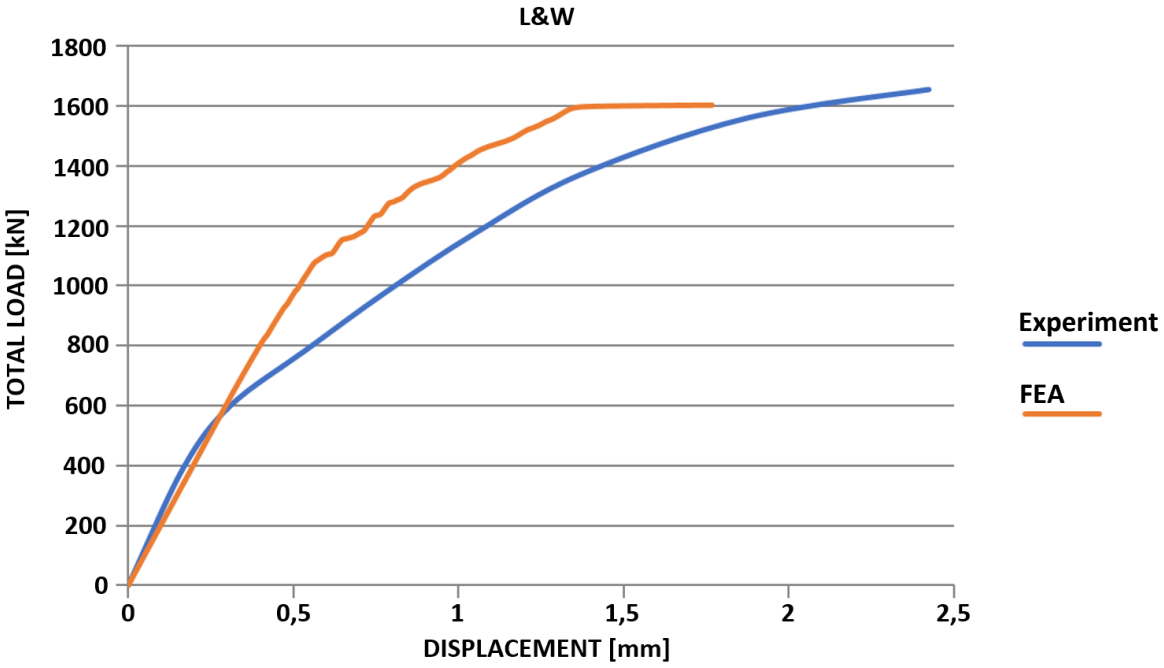

Figure 18 *Load-displacement curves according to test experiment and Abaqus analysis for the L&W deep beam*

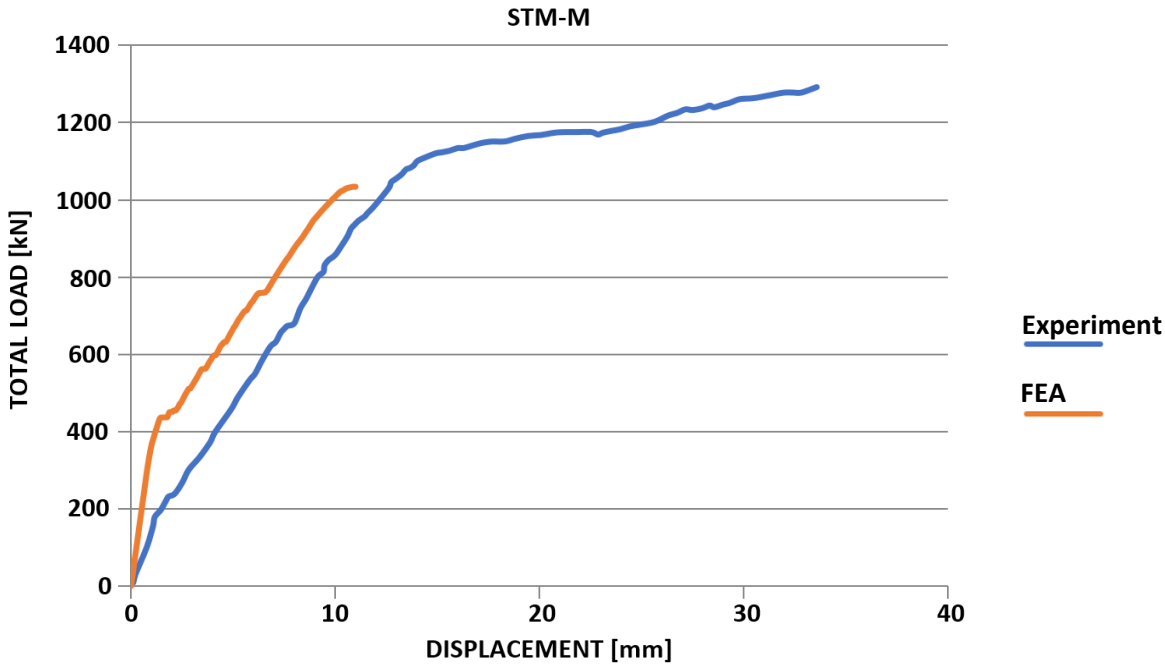

Figure 19 *Load-displacement curves according to test experiment and Abaqus analysis for the STM-M deep beam*

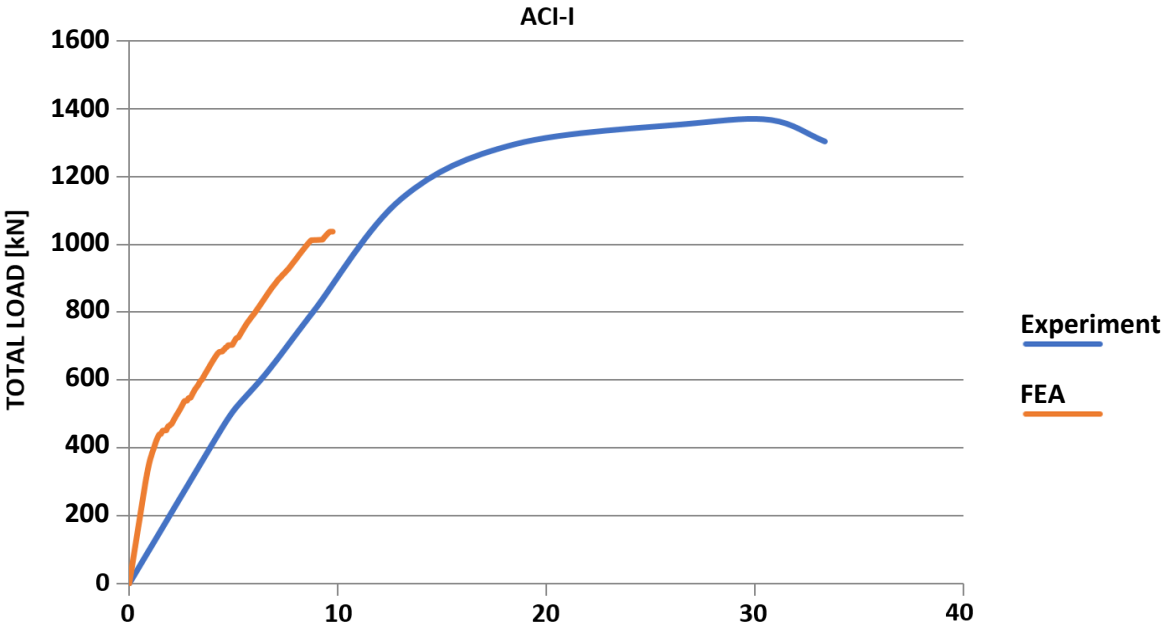

Figure 20 *Load-displacement curves according to test experiment and Abaqus analysis for the ACI-I deep beam*

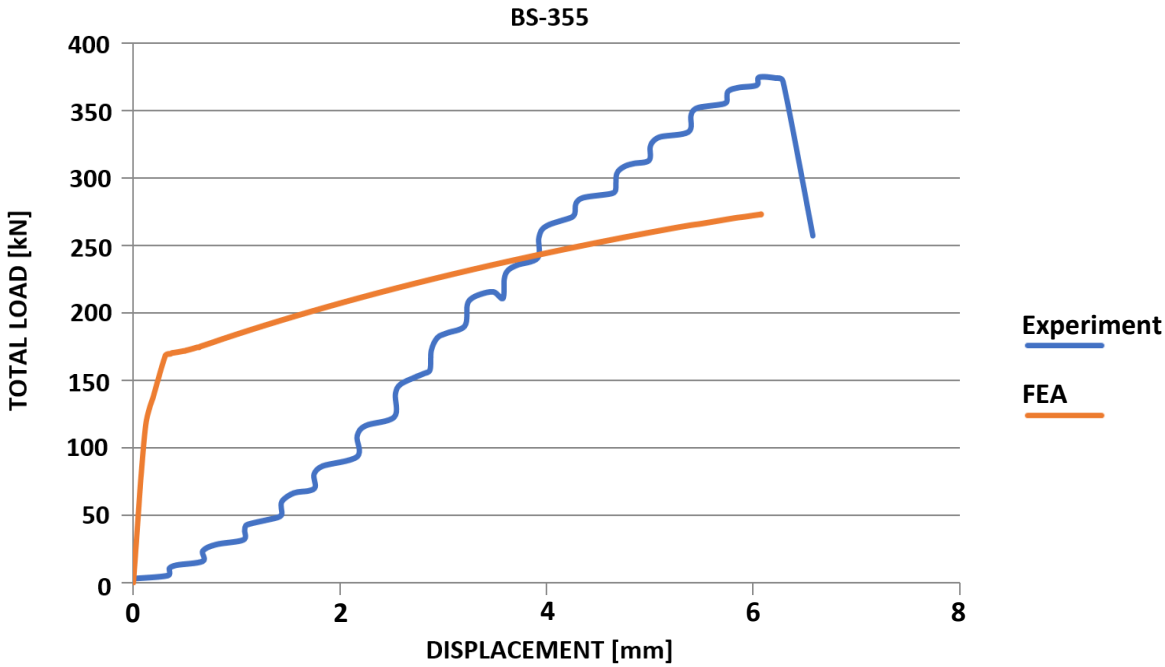

Figure 21 *Load-displacement curves according to test experiment and Abaqus analysis for the BS-355 deep beam*

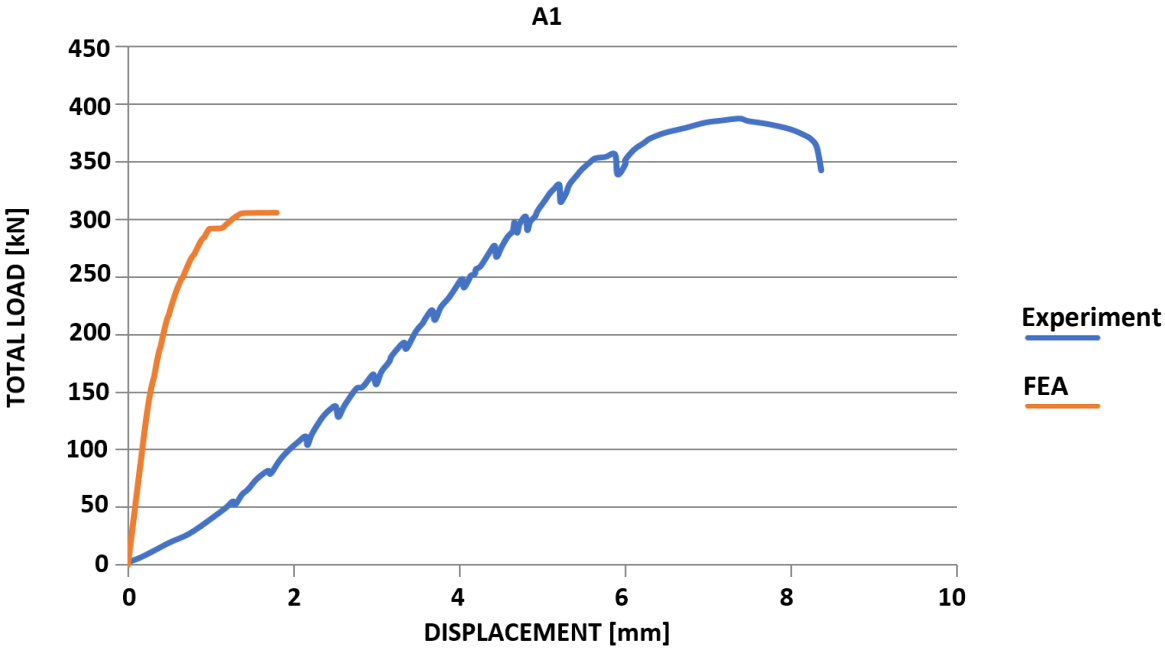

Figure 22 *Load-displacement curves according to test experiment and Abaqus analysis for the A1 deep beam*

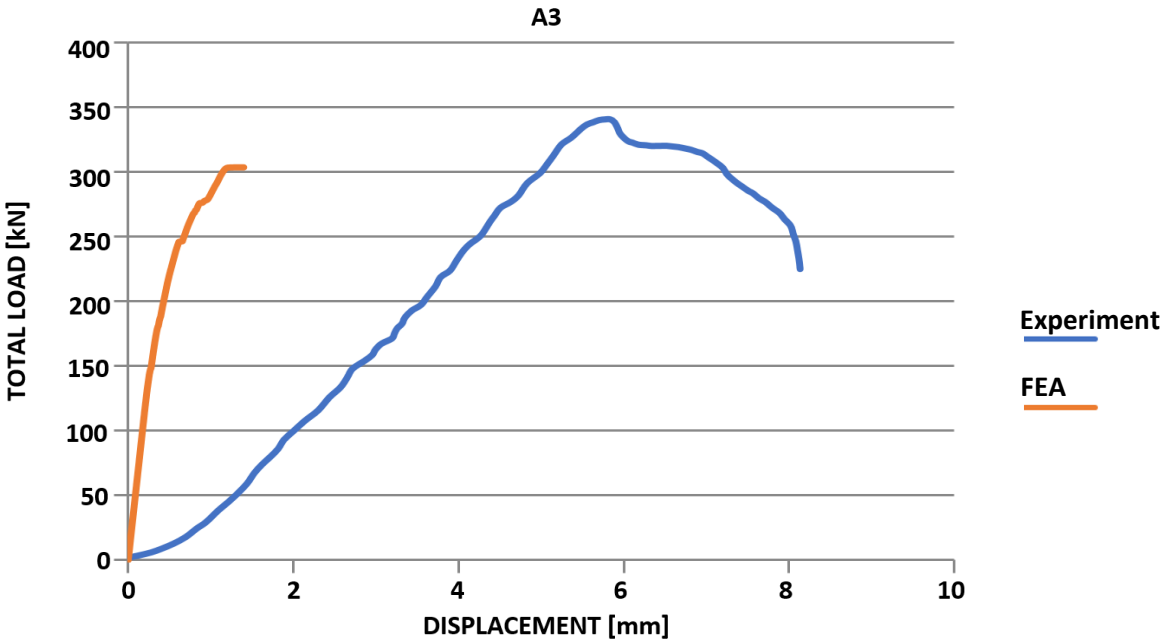

Figure 23 *Load-displacement curves according to test experiment and Abaqus analysis for the A3 deep beam*

5 Discussion

In this study, three main points of discussion must be made. First, the findings related to the aims and objectives mentioned in the introduction chapter, like the merits of the different structural analysis methods. Second, the results and how they hold up. And finally, several issues encountered and additional investigations made during the study process are presented and reviewed.

5.1 Comparison of different analysis methods

Based on the literature review and the results of the structural analyses, comparisons between the different analysis methods can be made and several different attributes determined. For the sake of simplicity, these attributes were separated into advantages and disadvantages.

5.1.1 Sectional analysis method

Advantages

To start, the procedure for sectional analysis is relatively straightforward. One needs just enough information to calculate, using simple equilibrium, the distribution of forces over the span of the beam, as well as the geometry and reinforcement layout of the beam's sections of interest required to determine the strain-stress distribution (and accompanying forces) across the cross-section. Due to their simplicity, the calculations needed were, compared to other structural analysis methods, both simple to compute and easy to find in literature. For beams with typical sectional geometries, they can be found almost entirely in EC2. The lack of complicated aspects makes the sectional analysis method easy to perform quickly using simple means. In conventional beam cases, it is often enough to use pen and paper.

Disadvantages

Though sectional analysis is applicable in practice under a lot of circumstances, it is important to note that it makes several assumptions that do not strictly correspond with reality. For example, that plane sections remain plane after deformation. It follows that one cannot typically use sectional analysis to model D-regions, where the assumption of plane sections remaining plane is often incorrect. This extends to deep beams, where the entire beam is a D-region. In the study, this can be seen in the sectional analysis procedure and results of the studied deep beams, see Figure 15. The best example is that of the L&W deep beam. To start, the sectional analysis results, especially the shear capacity, does not approach the one found in the experiments, as can be expected. Due to the discrepancy between these results, it is not unreasonable to deduce that the load capacity according to sectional analysis is not representative of the actual capacity and that the deeper the beams the larger the disparity between the results. A note should be made about the use of sectional analysis and whether it is applicable to some of the higher deep beams at all. For example, what was found when analyzing the L&W deep beam using the sectional analysis method was that it couldn't account for the abnormally large height of the deep beam. The design codes advised to check shear capacity in a section at a distance equal to the inner lever arm from the inner edge of the support. This would put the considered section inside the opposite support. Instead, the section right next to the inner support edge was used, see Appendix A.

5.1.2 Strut-and-tie method

Advantages

One of the most positive attributes of the STM is its wide range of applicability. It can be used to model almost all reinforced concrete designs, not just B-regions but also, more importantly for the scope of this study, D-regions as well. Similarly to sectional analysis, little information is needed to apply STM. For example, the information needed for designing the arrangements of reinforcement in deep beams include dimensions, material properties (concrete and steel) and design load. Consequently, it is a very quick an easy method, to the extent that one can perform it by hand calculations alone, at least when dealing with simple models like simply supported beams of conventional geometry. In this study, this can be seen with the results displayed in Figure 16, where the capacities according to STM come quite close to those in the experiments. The result of STM compared to the test experiments are 92% on average—excepting the BS-355 beam, which was quite different in its application of loads from the other beams and required special assumptions to be made—and this can be accounted for with the fact that, even in experiments, there are certain margins of error and experiments with the same inputs and circumstances can yield different results over multiple iterations. Thus, it is reasonable to consider the results between STM analyses and experiments to fall within the equitable margins.

Disadvantages

STM requires some assumptions that are based on idealizations in theory of plasticity on which STM is based. Meaning, the materials are assumed to be ideally plastic. This means that STM is limited to ULS, where plastic deformations can develop, and it is not applicable for design in SLS. In reality, the materials have a limited plastic deformation also in ULS whereas STM assumes an unlimited plastic deformation capacity. Finally, the strut angle is assumed and there are multiple ways STM could be applied even for just a singular beam and one must make a choice as to which is the most plausible using, for example, force path method or linear elastic analysis. A major downside of STM is that it is, typically, only suited for ULS and not SLS.

5.1.3 Finite element analysis

Advantages

The main advantage of the non-linear FEA method is that it can, potentially, come the closest to capturing the real response of the structure. Certainly, it can do better than the simpler methods. In this study, specifically, its results best approached those of the test experiments in four of the six beams (STM performing slightly better for ACI-I and better for A1), see Section 4. It is even possible to accurately predict the behavior in structures with irregular geometric shapes with relatively simple adjustments. Another very positive attribute is that non-linear FEA, specifically with results achieved by a simulation program, can show the results not just numerically, but also as graphs and figures. Meaning, it is possible to study, for example, the development of stress, strain, and displacements over the entire load duration. This is something very useful that’s not practically possible with the other structural analysis methods.

Disadvantages

The main disadvantage of non-linear FEA methods is how, when compared to the other structural analysis methods, time consuming they are. They are also not well suited for a design situation. This is both because only chosen forms can be analyzed and because of the difficulty of verifying and evaluating the analyses automatically regarding load-bearing capacity in ULS. This difficulty is in part because of convergence problems. Another disadvantage is that using non-linear FEA requires a computer program. Even when such software is available, though, there are still issues unique to non-linear FEA. Firstly, it demands more decision making on the part of the engineer. This includes more material model parameters than used in other methods. Also, parts of the model, like supports, need consideration and careful modelling. Additionally, one must choose the right finite elements and an appropriate mesh size. If this isn't done, then there's a risk that no results are obtained or, even worse, that the accrued results are inaccurate and lead to a false sense of security regarding the performance of the analyzed beam. Even small differences in the input can lead to vastly different results. For examples of such instances over the course of this study, see Chapter 5.3.

5.1.4 Summary

Evidently, each method has its own advantages and disadvantages. They are summarized in Table 5 below.

Structural analysis method	Advantages	Disadvantages
Sectional analysis	• Straightforward • Calculations steps easy to find and implement	• Assumes plane sections remain plane • Not usable for deep beams
STM	• Wide applicability • Simple to use • Little information needed	• Relies on assumptions, like ideally plastic materials • Usable for ULS but not SLS
Non-linear FEA	• Very precise and accurate • Possible to review many outputs simultaneously • Can study progression of behavior over increased loading, displacement, etc.	• Requires an FEA-based simulation program • Involves a lot of decision-making for the engineer • Results are sensitive to small differences in input

Table 5 Summary of the advantages and disadvantages of the different structural analysis methods.

5.2 Accuracy and significance of results

Important to understand about this study is that, since all the models deal with approximations, the results are not very precise. For example, sectional analysis assumes plane sections remain plane—something not true for deep beams—STM assumes ideally plastic materials, and non-linear FEA is sensitive enough that small changes in the inputs might lead to large differences in results. Thus, the results should be interpreted more as estimates than as precise figures. In addition, the limited number of deep beams tested lend the results a modest level of significance. Ideally, a solid number of deep beams for each variety of height and load condition should have been used. However, the study was limited to a few different deep beams, previously tested and reported in the literature. Several of the beams studied had a high width-to-height ratio and were symmetrical, with a four-point bending load configuration, and the results for this kind of deep beams are judged to be significant. There are, however, also other sorts of deep beams. Deep beams with a very low width-to-height ratio, asymmetrical, or under a distributed or three-point bending load. For these kinds, there are only one example each. So, for these kinds of deep beams, the results are less significant. However, one can, based on the results, talk about the trends of deep beam behavior in general. Finally, the results agree with the literature, but with some caveats, especially for the non-linear FEA method, which runs into convergence problems. This could be improved by further testing and study of the inputs and the effects of increased complexity of simulation models. Additionally, something to note about the load-displacement curves based on the non-linear FE analyses, derived from Abaqus, is that they behave differently, especially at the start, from those based on the test experiments, see Section 4.3.1. In the experiments, the load-displacement curves have a nearly horizontal start with an initially positive acceleration of the slope. Conversely, in Abaqus, the curves ascend quickly and accelerates negatively. This disparity can be explained when softening of some of the parts involved in the test experiments is considered.

5.3 Additional remarks on finite element analysis

Supplementary investigations were made to better determine the effects of various Abaqus inputs. These include analyzing bond-slip implementation, meshing size, size of the viscosity factor, inclusion of geometric nonlinearity, the use of combined or separate main tensile reinforcement bars, and the difference between tying and not tying the horizontal and vertical lines of reinforcement. The results of these investigations informed and verified several modeling choices.

6 Conclusions and further studies

6.1 Conclusions

In this study, several different matters were investigated. Firstly, what the advantages and disadvantages of the sectional analysis, STM, and non-linear FEA structural analysis methods were in determining the load capacity and behavior of deep beams. Also, the methods were to be compared with one another in terms of accuracy and ease of implementation. The obtained results were enough to answer the questions while still leaving open the possibility for future studies to delve further into the related issues.

The sectional analysis method was found to be an easy and time efficient method of structural analysis. Yet, the disparity of results between the sectional analysis and the experiments proved it to be of limited use when it came to application for deep beams. For example, the total load capacity calculated were significantly different from those demonstrated in lab tests. Another aspect to consider is the character, specifically the height, of the beam analyzed. The results indicate that the higher, i.e. deeper, the beam, the greater the disparity of results between sectional analysis and experiments.

By contrast, the STM method was found to be significantly more useful. Its results were markedly closer to those from the experiments. The method was also quick and straightforward to use, even with relatively simple means. The non-linear FEA, however, was quite complicated, with a lot of set-up and a wide array of difference in the final results even with slight differences in input data.

When comparing these three methods, it becomes clear that the STM and non-linear FEA methods were the most accurate. Similarly, it is apparent that the sectional analysis and STM methods were the quickest and easiest methods to use. The FEA was quite tricky to use correctly for some of the cases and investigations into several input parameters were needed to improve the results. Thus, it can be concluded that it is a poor idea to trust at least the initial results of non-linear FEA blindly. Preferably, a verification of the finite element model is needed first.

Thus, the findings of this study indicate that, if the aim is to analyze deep beams, then it is recommended to start by making a quick and easy initial analysis using a relatively simple method like STM. For deep beams, traditional structural analyses are fine to forego. Finally, if a more precise figure is required or if the behavior over load increase is of interest, then it is a good idea to test the deep beam in an FEA based simulation program. However, one should keep in mind that the non-linear FEA method is sensitive to changes in input values and small differences could lead to very different results. One way to avoid this is to reduce the model's complexity as much as can be done without losing the beam's overall character.

6.2 Further studies

To achieve greater understanding of the subject of this study, more studies can be made in the future. Some ways to do this are to fill the gaps in the current state of the study or to take them further. Some examples of this is to find the best way of modeling bond-slip in Abaqus or to investigate the differences in results, using identical input data, obtained when using different FEA simulation programs—like Abaqus, Diana, or COMSOL—to model the behavior of deep beams.

There is, of course, the possibility of raising the significance of the results by replicating the research and to apply the tests to more deep beams of the same or different character than used in this study. For example, to investigate how the different design codes (EC2 and ACI, for instance) compare to each other and the results of the experiments. Another avenue for future is to expand the scope of the study. For example, to make the same investigation, but taking the SLS and not just ULS into account.

7 References

Abdelrahman, A., Tadros, G. and Rizkalla, S. H. (2003) 'Experimental Evaluation of Design Procedures for Shear Strength of Deep Reinforced Concrete Beams', *Aci Structural Journal*, 19(99), pp. 595–604. Available at: http://www.concrete.org/PUBS/JOURNALS/OLJDetails.asp?ID=51663392.

ACI 318-08 (2008) *Building Code Requirements for Structural Concrete (ACI 318-08) and Commentary - An ACI Standard*. 318th-08 edn, *American Concrete Institute*. 318th-08 edn. Edited by A. C. 318. Farmington Hills, USA.

Al-Emrani, M. *et al.* (2011) *Bärande konstruktioner Del 2*. Göteborg, Sverige 2011: CHALMERS UNIVERSITY OF TECHNOLOGY.

Al-Emrani, M. *et al.* (2013) *Bärande konstruktioner Del 1*. Göteborg, Sverige 2013: CHALMERS UNIVERSITY OF TECHNOLOGY.

Birgisson, S. R. (2011) *SHEAR RESISTANCE OF REINFORCED CONCRETE Thesis in Civil Engineering BSc*.

EN 1992-1-1 (2004) 'Eurocode 2: Design of concrete structures - Part 1-1 : General rules and rules for buildings', *British Standards Institution*, 1(2004), p. 230. doi: [Authority: The European Union Per Regulation 305/2011, Directive 98/34/EC, Directive 2004/18/EC].

Engström, B. (2015) *Design and analysis of deep beams, plates and other discontinuity regions*. 2015th edn. Göteborg, Sweden 2015: CHALMERS UNIVERSITY OF TECHNOLOGY.

fib (2013) *Model Code for Concrete Structures 2010*. International Federation for Structural Concrete (fib). doi: 10.1002/9783433604090.

Kong, F. . (2002) *Reinforced Concrete Deep Beams*. Edited by F. . Kong.

Li, X. (2007) *Finite Element Modeling Of Skewed Reinforced Concrete Bridges And The Bond-Slip Relationship Between Concrete And Reinforcement*. Auburn University.

Mario Plos (1996) *Finite element analysis of reinforced concrete structures*. Göteborg, Sweden 2000: CHALMERS UNIVERSITY OF TECHNOLOGY.

Panjehpour, M. *et al.* (2012) 'An Overview of Strut-and-Tie Model and its Common Challenges', *International Journal of Engineering Research in Africa*, 8, pp. 37–45. doi: 10.4028/www.scientific.net/JERA.8.37.

Quintero-Febres, C. G., Parra-Montesinos, G. and Wight, J. K. (2006) 'Strength of struts in deep concrete members designed using strut-and-tie method', *ACI Structural Journal*, pp. 577–586.

Sam-Young, N., Chang-Yong, L. and Kyeong-Min, L. (no date) *Deep Beam Design Using Strut-Tie Model*. Ansan, Korea.

Vecchio, F. J. (1989) 'Nonlinear finite element analysis of reinforced concrete membranes', *ACI Structural Journal*, pp. 26–35. doi: 10.1680/stco.2.4.201.40356.

Wang, D. J. *et al.* (2013) 'Review of the Application of Finite Element Model Updating to Civil Structures', *Key Engineering Materials*, 574, pp. 107–115. doi: 10.4028/www.scientific.net/KEM.574.107.

APPENDIX A

Cells in tables with a darker background color are values directly from the source while others are either estimates based on the source or estimated standard values.

BEAM	ϕ (mm)	$s_{critical}$ (mm)	n_{span}	$A_{s,main}$ (mm²)
BS-335	16	50*	4	804
L&W	8,3	60*	8	432
STM-M	32,3	44,5*	6	3054 (509 per rebar)
ACI-I	32,3	44,5*	6	3054 (509 per rebar)
A1	22,2	90	4	1550
A3	22,2	90	4	1550

* estimated

BEAM	ϕ (mm)	$s_{critical}$ (mm)	n_{span}	$A_{s,secondary}$ (mm²)
BS-335	-	-	-	-
L&W	5	260	12	236 (19,5 per rebar)
STM-M	32,3	260	2	1639 (819 per rebar)
ACI-I	9,51	260	12	852 (71 per rebar)
A1	12,7/6,4	90	2/2	318 (127/32 per rebar)
A3	12,7	90	2	254 (127 per rebar)

* estimated

n_{span} and $A_{s,shear}$ is the number of reinforcement bars and total cross-sectional area of the reinforcement in the full span. $S_{critical}$ is the distance between lines of stirrups in the critical span.

BEAM	ϕ (mm)	$s_{critical}$ (mm)	n_{span}	$A_{s,shear}$ (mm²)
BS-335	-	-	-	-
L&W	5	260	14	275 (19,5 per rebar)
STM-M	9,51	150	32	2273 (71 per rebar)
ACI-I	9,51	150	56	3978 (71 per rebar)
A1	6,38	135	60	1918 (192 per rebar)
A3	-	-	-	-

n_{span} and $A_{s,shear}$ is the number of reinforcement bars and total cross-sectional area of the reinforcement in the full span. $S_{critical}$ is the distance between lines of stirrups in the critical span.

BEAM	LENGTH (mm)	WIDTH (mm)	HEIGHT (mm)	EFFECTIVE DEPTH (mm)	A_c (mm²)
BS-335	1250	200	335	307	$67 \cdot 10^3$
L&W	1600	100	1600	1485	$160 \cdot 10^3$
STM-M	4470	305	915	813	$279 \cdot 10^3$
ACI-I	4470	305	915	813	$279 \cdot 10^3$
A1	2440	150	460	370	$69 \cdot 10^3$
A3	2440	150	460	370	$69 \cdot 10^3$

A_c is the cross-sectional area of the concrete, $A_c = \text{WIDTH} \cdot \text{HEIGHT}$

BEAM	$f_{y,main}$ (MPa)	$f_{y,shear}$ (MPa)	$f_{y,secondary}$ (MPa)	$f_{concrete}$ (MPa)
BS-335	530 (measured)	-	-	31,43 (measured)
L&W	415	415	415	29,6
STM-M	420 (measured)	450 (measured)	450 (measured)	28 (measured)
ACI-I	420 (measured)	450 (measured)	450 (measured)	33 (measured)
A1	462 (assumed)	407 (assumed)	455 (assumed)	22 (measured)
A3	462 (assumed)	-	455 (assumed)	22 (measured)

assumed = strength assumed based on grade ordered
measured = experimentally measured

BS-335

(Vecchio, 1989)

[mm]

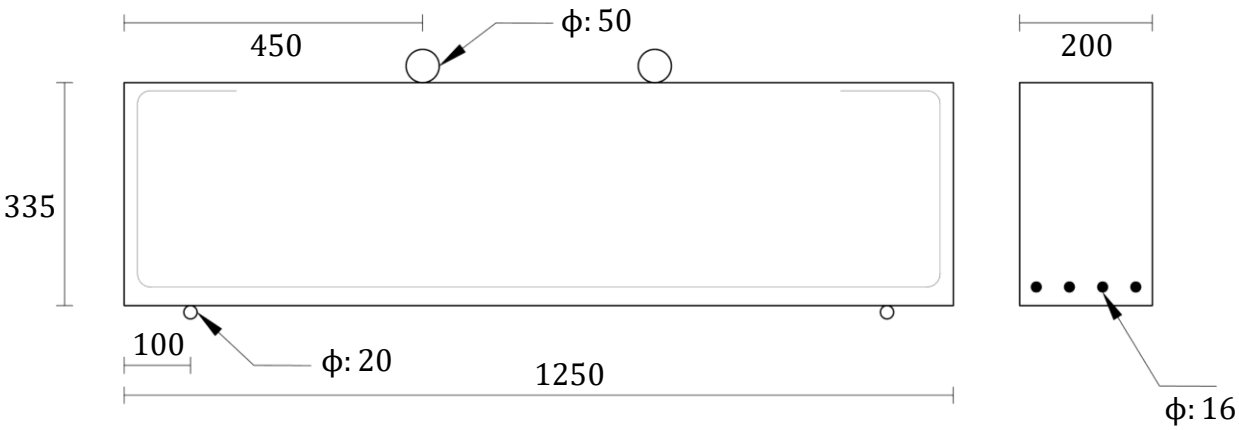

- Longer beam
- Symmetrical
- No shear reinforcement
- Load applied through rollers
- Supported on rollers

MESH

	MESHED PART			
	BEAM	**PRESSURE ROLLER**	**SUPPORT ROLLER**	**REINFORCEMENT**
MESH SIZE	0.0125	0.0071	0.015	0.0028

MATERIAL PROPERTIES

CONCRETE

DENSITY

MASS DENSITY $[kg/m^3]$
2400

ELASTIC

YOUNG'S MODULUS [GPa]	**POISSON'S RATIO**
33	0.2

CONCRETE DAMAGE PLASTICITY

PLASTICITY				
DILATION ANGLE	**ECCENTRICITY**	**fb0/fc0**	**K**	**VISCOSITY PARAMETER**
35	0.1	1.16	0.67	1e-7
COMPRESSIVE BEHAVIOR				
YIELD STRESS [MPa]	**INELASTIC STRAIN**			
31.43/31.5	0/1			
TENSILE BEHAVIOR				
YIELD STRESS [MPa]	**FRACTURE ENERGY [MPa]**			
5	136			

STEEL (tensile rebars)

DENSITY

MASS DENSITY [kg/m^3]
7850

ELASTIC

YOUNG'S MODULUS [GPa]	**POISSON'S RATIO**
200	0.3

PLASTIC

YIELD STRESS [MPa]	**PLASTIC STRAIN**
530/637.5	0/0.048

STEEL (support/pressure roller)

DENSITY

MASS DENSITY $[\mathbf{kg/m^3}]$
7850

ELASTIC

YOUNG'S MODULUS [**GPa**]	**POISSON'S RATIO**
$200 \cdot 10^3$	0.3

REMARKS/SIMPLIFICATIONS

- In STM, the circular load application and support elements were considered squares, with the width and height the same as the circular elements' diameter.

A1

(Quintero-Febres, Parra-Montesinos and Wight, 2006)

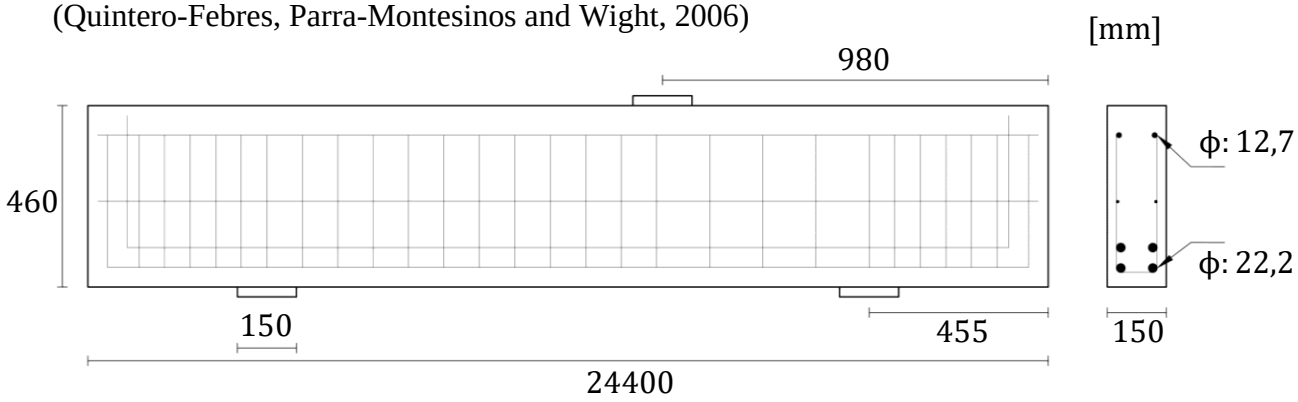

- Longer beam
- Asymmetrical
- Concentrated load
- Considerable shear reinforcement

MESH

	MESHED PART			
	BEAM	**PLATES**	**V. REBARS**	**H. REBARS**
MESH SIZE	0.03	0.015	0.03	0.03

MATERIAL PROPERTIES

CONCRETE

DENSITY

MASS DENSITY $[kg/m^3]$
2400

ELASTIC

YOUNG'S MODULUS [GPa]	**POISSON'S RATIO**
33	0.2

CONCRETE DAMAGE PLASTICITY

PLASTICITY				
DILATION ANGLE	**ECCENTRICITY**	**fb0/fc0**	**K**	**VISCOSITY PARAMETER**
35	0.1	1.16	0.67	1e-7
COMPRESSIVE BEHAVIOR				
YIELD STRESS [MPa]	**INELASTIC STRAIN**			
22/22.5	0/1			
TENSILE BEHAVIOR				
YIELD STRESS [MPa]	**FRACTURE ENERGY [MPa]**			
5	127			

STEEL (tensile)

DENSITY

MASS DENSITY $[kg/m^3]$
7850

ELASTIC

YOUNG'S MODULUS [GPa]	**POISSON'S RATIO**
200	0.3

PLASTIC

YIELD STRESS [MPa]	**PLASTIC STRAIN**
462/462.5	0/0.048

STEEL (plate)

DENSITY

MASS DENSITY $[\mathbf{kg/m^3}]$
7850

ELASTIC

YOUNG'S MODULUS [**GPa**]	**POISSON'S RATIO**
$200 \cdot 10^3$	0.3

STEEL (vertical rebars)

DENSITY

MASS DENSITY $[\mathbf{kg/m^3}]$
7850

ELASTIC

YOUNG'S MODULUS [**GPa**]	**POISSON'S RATIO**
200	0.3

PLASTIC

YIELD STRESS [**MPa**]	**PLASTIC STRAIN**
441/441.5	0/0.048

STEEL (vertical rebars in critical shear span, horizontal rebars in midsection)

DENSITY

MASS DENSITY $[kg/m^3]$
7850

ELASTIC

YOUNG'S MODULUS [GPa]	**POISSON'S RATIO**
200	0.3

PLASTIC

YIELD STRESS [MPa]	**PLASTIC STRAIN**
407/407.5	0/0.048

STEEL (horizontal rebars in top of section)

DENSITY

MASS DENSITY $[kg/m^3]$
7850

ELASTIC

YOUNG'S MODULUS [GPa]	**POISSON'S RATIO**
200	0.3

PLASTIC

YIELD STRESS [MPa]	**PLASTIC STRAIN**
455/455.5	0/0.048

A3

(Quintero-Febres, Parra-Montesinos and Wight, 2006)

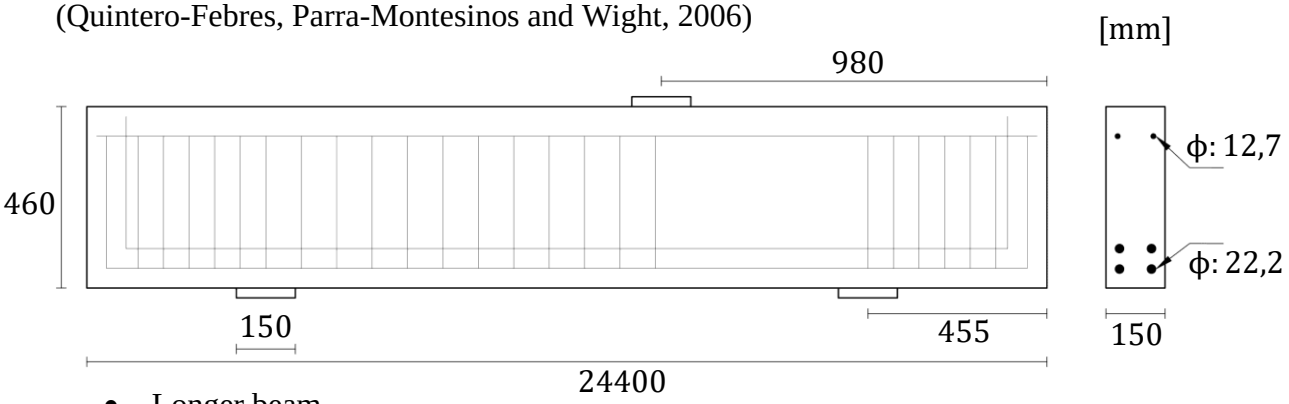

- Longer beam
- Asymmetrical
- Concentrated load
- Considerable shear reinforcement

MESH

	MESHED PART			
	BEAM	**PRESSURE/SUPPORT PLATE**	**Ve. REBARS**	**Ho. REBARS**
MESH SIZE	0.03	0.015	0.03	0.03

MATERIAL PROPERTIES

CONCRETE

DENSITY

MASS DENSITY $[kg/m^3]$
2400

ELASTIC

YOUNG'S MODULUS [GPa]	**POISSON'S RATIO**
33	0.2

CONCRETE DAMAGE PLASTICITY

PLASTICITY				
DILATION ANGLE	**ECCENTRICITY**	**fb0/fc0**	**K**	**VISCOSITY PARAMETER**
35	0.1	1.16	0.67	1e-7
COMPRESSIVE BEHAVIOR				
YIELD STRESS [MPa]	**INELASTIC STRAIN**			
22/22.5	0/1			
TENSILE BEHAVIOR				
YIELD STRESS [MPa]	**FRACTURE ENERGY [MPa]**			
3.3	127			

STEEL (tensile)

DENSITY

MASS DENSITY $[kg/m^3]$
7850

ELASTIC

YOUNG'S MODULUS [GPa]	**POISSON'S RATIO**
200	0.3

PLASTIC

YIELD STRESS [MPa]	**PLASTIC STRAIN**
462/462.5	0/0.048

STEEL (plate)

DENSITY

MASS DENSITY $[\mathbf{kg/m^3}]$
7850

ELASTIC

YOUNG'S MODULUS [**GPa**]	**POISSON'S RATIO**
$200 \cdot 10^3$	0.3

STEEL (vertical rebars)

DENSITY

MASS DENSITY $[\mathbf{kg/m^3}]$
7850

ELASTIC

YOUNG'S MODULUS [**GPa**]	**POISSON'S RATIO**
200	0.3

PLASTIC

YIELD STRESS [**MPa**]	**PLASTIC STRAIN**
441/441.5	0/0.048

STEEL (horizontal rebars in top of section)

DENSITY

MASS DENSITY $[kg/m^3]$
7850

ELASTIC

YOUNG'S MODULUS [**GPa**]	**POISSON'S RATIO**
200	0.3

PLASTIC

YIELD STRESS [**MPa**]	**PLASTIC STRAIN**
455/455.5	0/0.048

ACI-I

(Abdelrahman, Tadros and Rizkalla, 2003)

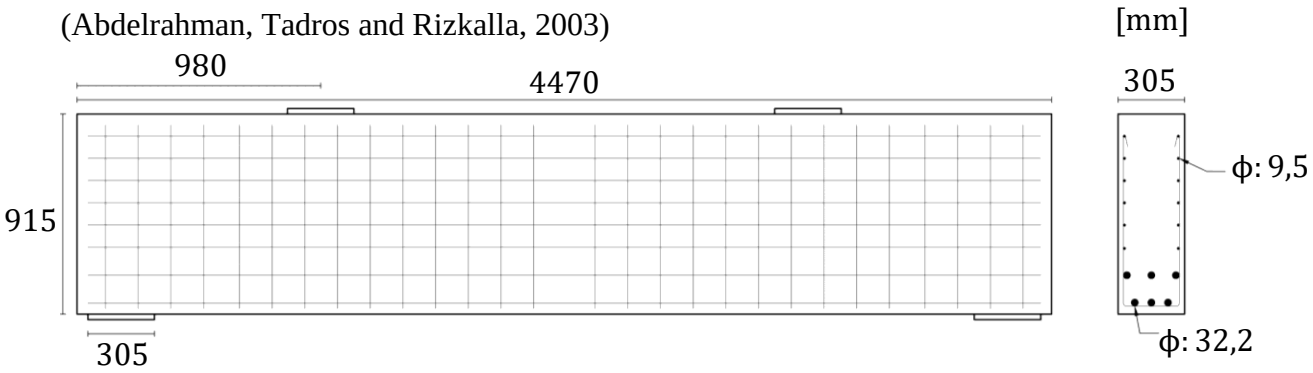

- Longer beam
- Symmetrical
- Concentrated load
- Lots of shear and horizontal reinforcement (web reinforcement)

MESH

	MESHED PART			
	BEAM	**PLATES**	**V. REBARS**	**H. REBARS**
MESH SIZE	0.025	0.03	0.03	0.03

MATERIAL PROPERTIES

CONCRETE

DENSITY

MASS DENSITY [kg/m^3]
2400

ELASTIC

YOUNG'S MODULUS [GPa]	**POISSON'S RATIO**
33	0.2

CONCRETE DAMAGE PLASTICITY

PLASTICITY				
DILATION ANGLE	**ECCENTRICITY**	**fb0/fc0**	**K**	**VISCOSITY PARAMETER**
35	0.1	1.16	0.67	1e-7
COMPRESSIVE BEHAVIOR				
YIELD STRESS [MPa]	**INELASTIC STRAIN**			
33/33.5	0/1			
TENSILE BEHAVIOR				
YIELD STRESS [MPa]	**FRACTURE ENERGY [MPa]**			
5	137			

STEEL (tensile)

DENSITY

MASS DENSITY $[kg/m^3]$
7850

ELASTIC

YOUNG'S MODULUS [GPa]	**POISSON'S RATIO**
200	0.3

PLASTIC

YIELD STRESS [MPa]	**PLASTIC STRAIN**
420/700	0/0.048

STEEL (plate)

DENSITY

MASS DENSITY $[\mathbf{kg/m^3}]$
7850

ELASTIC

YOUNG'S MODULUS [**GPa**]	**POISSON'S RATIO**
$200 \cdot 10^3$	0.3

STEEL (vertical & horizontal rebars)

DENSITY

MASS DENSITY $[\mathbf{kg/m^3}]$
7850

ELASTIC

YOUNG'S MODULUS [**GPa**]	**POISSON'S RATIO**
200	0.3

PLASTIC

YIELD STRESS [**MPa**]	**PLASTIC STRAIN**
450/720	0/0.048

STM-M

(Abdelrahman, Tadros and Rizkalla, 2003)

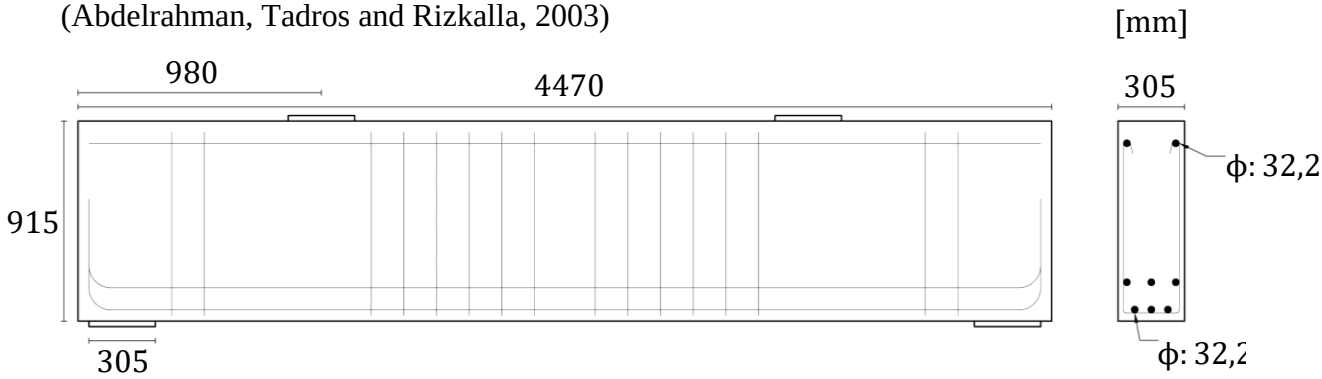

- Longer beam
- Symmetrical
- Concentrated load
- Little shear reinforcement in critical section

MESH

	MESHED PART			
	BEAM	**PLATE**	**V. REBARS**	**H. REBARS**
MESH SIZE	0.025	0.03	0.03	0.03

MATERIAL PROPERTIES

CONCRETE

DENSITY

MASS DENSITY $[kg/m^3]$
2400

ELASTIC

YOUNG'S MODULUS [GPa]	**POISSON'S RATIO**
33	0.2

CONCRETE DAMAGE PLASTICITY

PLASTICITY				
DILATION ANGLE	**ECCENTRICITY**	**fb0/fc0**	**K**	**VISCOSITY PARAMETER**
35	0.1	1.16	0.67	1e-7
COMPRESSIVE BEHAVIOR				
YIELD STRESS [MPa]	**INELASTIC STRAIN**			
28	0			
TENSILE BEHAVIOR				
YIELD STRESS [MPa]	**FRACTURE ENERGY [MPa]**			
5	133			

STEEL (tensile)

DENSITY

MASS DENSITY $[kg/m^3]$
7850

ELASTIC

YOUNG'S MODULUS [GPa]	**POISSON'S RATIO**
$200 \cdot 10^3$	0.3

PLASTIC

YIELD STRESS [MPa]	**PLASTIC STRAIN**
420/700	0/0.048

STEEL (plate)

DENSITY

MASS DENSITY $[kg/m^3]$
7850

ELASTIC

YOUNG'S MODULUS [GPa]	**POISSON'S RATIO**
$200 \cdot 10^3$	0.3

STEEL (vertical & horizontal)

DENSITY

MASS DENSITY $[kg/m^3]$
7850

ELASTIC

YOUNG'S MODULUS [GPa]	**POISSON'S RATIO**
200	0.3

PLASTIC

YIELD STRESS [MPa]	**PLASTIC STRAIN**
450/720	0/0.048

L&W

(Vecchio, 1989) [mm]

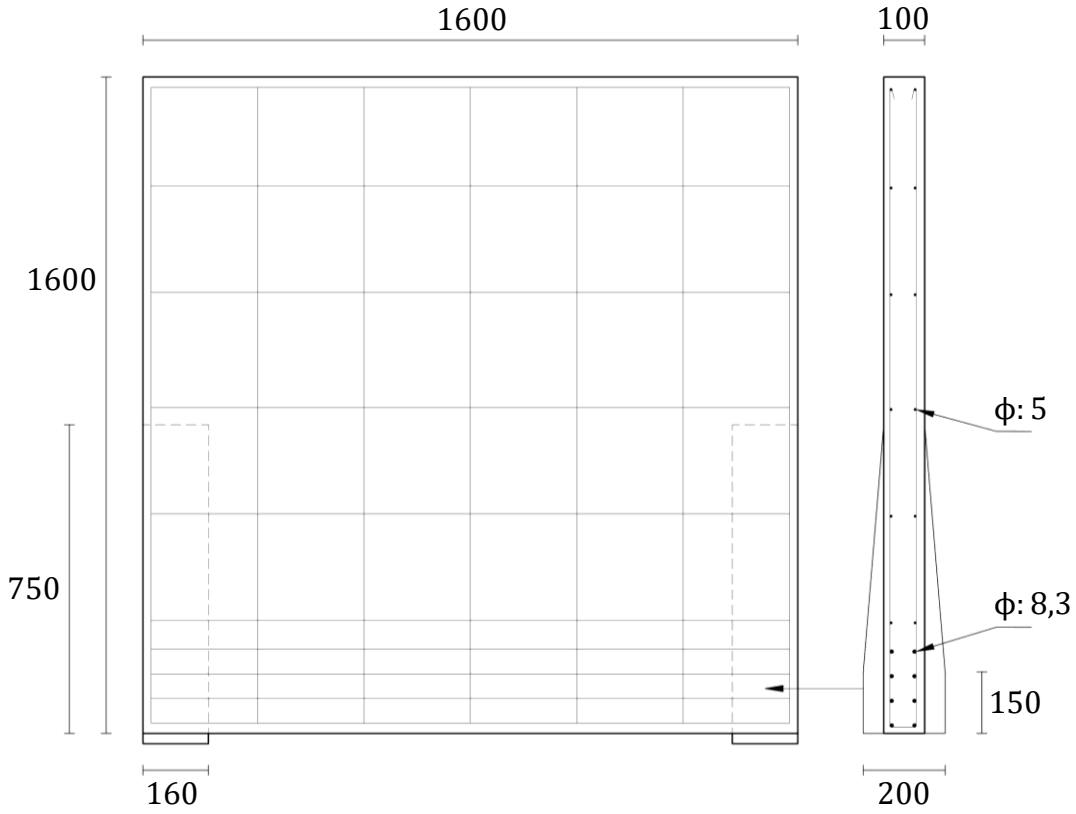

- Wall-like
- Distributed load
- Symmetrical
- Shear reinforcement
- Extra wide supports

MESH

	MESHED PART			
	BEAM	**PLATES**	**V REBARS**	**H. REBARS**
MESH SIZE	0.04	0.02	0.03	0.03

MATERIAL PROPERTIES

CONCRETE

DENSITY

MASS DENSITY $[kg/m^3]$
2400

ELASTIC

YOUNG'S MODULUS [GPa]	**POISSON'S RATIO**
33	0.2

CONCRETE DAMAGE PLASTICITY

PLASTICITY				
DILATION ANGLE	**ECCENTRICITY**	**fb0/fc0**	**K**	**VISCOSITY PARAMETER**
35	0.1	1.16	0.67	1e-7
COMPRESSIVE BEHAVIOR				
YIELD STRESS [MPa]	**INELASTIC STRAIN**			
29.6/30	0/1			
TENSILE BEHAVIOR				
YIELD STRESS [MPa]	**FRACTURE ENERGY [MPa]**			
5	134			

STEEL (tensile/horizontal/vertical rebars)

DENSITY

MASS DENSITY $[\mathbf{kg/m^3}]$
7850

ELASTIC

YOUNG'S MODULUS [**GPa**]	**POISSON'S RATIO**
200	0.3

PLASTIC

YIELD STRESS [**MPa**]	**PLASTIC STRAIN**
415/415.5	0/0.048

STEEL (plate)

DENSITY

MASS DENSITY $[\mathbf{kg/m^3}]$
7850

ELASTIC

YOUNG'S MODULUS [**GPa**]	**POISSON'S RATIO**
$200 \cdot 10^3$	0.3

REMARKS/SIMPLIFICATIONS

- In sectional analysis, the height was so large that the length from the edge of the support plate at which one typically considers shear ($0.9 \cdot d$) fell outside the span of the beam, so the section right next to the edge of the support plate was considered instead.

- In Abaqus, the varying thickness of the concrete right above the support (see image) was simplified to a unified thickness of 200 m. The rest, similarly to reality, was modeled as 100 mm thick.